APPLICATION OF GEOPHYSICAL WELL-LOGS IN EXPLORATION FOR STRATIGRAPHIC TRAPS IN THE LAMU BASIN

By

Kandie Jemutai Risper

I/56/7432/2003

A Dissertation submitted in the partial fulfillment of the award of Masters of Science degree in Geology, University of Nairobi.

August, 2009

Declaration

I certify that the work carried in this report is wholly my effort and it has never been submitted nor published before except where references have been made to the various authorities therein.

Date---------- 5|5|0 9 ----------------------Signature---- ~~Kirathe~~ -------------------------------

Supervisor: Professor J. O. Barongo

        Associate professor

        Department of Geology

        University of Nairobi

Date---- 11|8|2009 ----------------Signature-----------------------------

Supervisor: Dr. D. W. Ichang'i

        Senior Lecturer

        Department of Geology

        University of Nairobi

Date---- 14th August 2009 -----Signature----------------------------

Abstract

World's oil and gas reserves are rapidly diminishing and they don't have to actually run out before precipitating a crisis. Predictions indicate that the peak and subsequent decline in world oil production will probably occur within the next few decades and as the demand for fossil fuel energy has increased dramatically over the past years, so has the necessity for more accurate methods of locating these deposits.

This research project the most promising method of application of geophysical well logs in the search for stratigraphic traps in the Lamu basin, including their use in correlation, location of facies change or pinch-out, analysis of subsurface resistivity fluids and determination of formation porosity and permeability.

Electric induction log was utilized which provided the data for evaluation of reservoir properties. In addition, the information from the log header was applied in the calculation of resistivity values of fluids. Necessary corrections were made on resistivity fluid values to formation temperature by the use of charts courtesy of Schlumberger well Services and Dresser Industries.

Processed lithologic well log data for the selected wells was utilized to generate fence diagram, which were effective in demonstrating changes in lithologic facies, pinch outs, unconformity and other stratigraphic conditions occurring in the basin thereby allowing inferences to be made on the location of stratigraphic types of traps in the Lamu basin.

Quantitative reservoir parameter evaluation results for the wells were obtained that indicate moderate to poor porosity

Acknowledgments

Abbreviations

a	-Tortuosity factor
BHT	-Bottom hole temperature
Rm	-Resistivity of drilling mud
Rmc	-Resistivity of mud cake
Rmf	-Resistivity of mud filtrates
Ro	-Resistivity of formations 100%water saturated
Rt	-Resistivity of uninvaded zone
Rw	-Resistivity of formation water
m	-Cementation exponents
Sw	-water saturations
SP	-Spontaneous potential
SSP	-Static spontaneous potential
ϕ-	-Porosity
F	-Formation factor
Lmst	- Limestone
Sst	-Sandstone
Fm	-Formations
Tsurf	-Temperature of the surface
T_f	.Temperature of formation

TABLE OF CONTENT

List of Figures

List of Tables

CHAPTER ONE

1.0 Introduction

1.1 General Background Information

The rate and scope of development science and technology have made heavy demands on oil and gas both as a source of fuel and energy and as the most essential raw material for chemical industry (Markoviskii, 1973). This has called for extensive search for such commodity and various exploration attempts have been made using techniques which are becoming continually more sophisticated to keep pace with the demands of modern hydrocarbon exploration

Geologists have classified petroleum traps into two basic types: structural traps and stratigraphic traps. Structural traps are traps that are formed because of a deformation in the rock layer that contains the hydrocarbons. Two common examples of structural traps are fault traps and anticlines. Stratigraphic traps are traps that result when the reservoir bed is sealed by other beds or by a change in porosity or permeability within the reservoir bed itself. The term stratigraphic trap was first coined by Levorsen, 1934, who defined a stratigraphic trap as "one in which the chief trap-making element is some variation in the stratigraphic lithology, or both, of the reservoir rock, such as a facies change, variable local porosity and permeability, or an up-structure termination of the reservoir rock, irrespective of the cause".

There are many different kinds of stratigraphic traps. In one type, a tilted or inclined layer of petroleum-bearing rock is cutoff or truncated by an essentially horizontal, impermeable rock layer.

Or sometimes a petroleum-bearing formation pinches out; that is, the formation is gradually cut off by an overlying layer. Another stratigraphic trap occurs when a porous

1

and permeable reservoir bed is surrounded by impermeable rock. Still another type occurs when there is a change in porosity and permeability in the reservoir itself. The upper reaches of the reservoir may be impermeable and nonporous, while the lower part is permeable and porous and contains hydrocarbons.

Presently, the main challenge in petroleum industry is to accrete reserves of oil and gas from stratigraphic prospects in order to meet the ever rising trend in energy demands of an expanding world population. Except for the offshore and certain frontier areas on land, many petroleum provinces of the world already have yielded their large structural accumulations to the conventional exploratory methods of geophysics, subsurface geology and field mapping (King, 1972)

In the past, the search for stratigraphic traps was so subjective: One of the main criteria in prospecting was the presence of favourable local structures in a potential or proved oil and gas basin (Markoviskii, 1973). Stratigraphic accumulations were discovered either as a result of testing structural prospects or by more or less random drilling. Even where stratigraphic prospects had definite potential, they commonly were not pursued successfully because of inadequate methods, improper evaluation of data and discouragement resulting from dry holes.

Prediction and subsequent discovery of economically important stratigraphic traps is a difficult scientific achievement which require utilization and integration of all available geological and geophysical information coupled with a sound geological reasoning and thorough understanding of the conditions necessary for the formation of stratigraphic traps. The concept of structure can neither be ignored nor separated from the search for

2

stratigraphic traps because the 3-D geometry of the trapping process of both types of accumulation.

Well logs play a particularly important role in providing a continuous record of a number of physical, chemical and electrical properties of rocks or fluids. Attributes such as density, resistivity and radioactivity of the rocks, which have been drilled through, are used to determine what types of rocks are in a well (Dobrin, 1960). Well logging denotes any operation wherein some characteristic data of the formation penetrated by a borehole are recorded in terms of depth. Such a record is called a log. In geophysical well logging, a probe is lowered in the well at the end of an insulated cable and physical measurements are performed and recorded in graphic forms as a function of depth. These records are called geophysical well logs, well logs or simply logs (George and Teh Fu Yen, 1976) Various types of measuring devices can be lowered in a borehole for the sole purpose of measuring (logging) both borehole and in-situ formation properties. These logging tools or logging sondes contain sensors that measure the desired down-hole properties, whether thermal, magnetic, electric, radioactive or acoustic. Insulated conductive cables not only lower these sondes into the borehole but also pass power to the sonde and transmit recorded signals (data) to the surface, where the latter are recorded as a log. Hence geophysical well logging methods provide a detailed and economic evaluation of the entire length of the drilled hole. It also provides the main keys to realistic formation evaluation and to determine the chemical, physical or chemical rock properties in-situ and the nature and the amount of fluids contained in the pore spaces thereby giving an indication of economic worth of the natural resources accumulated in the subsurface such as oil and gas

3

Exploration and exploitation of a prospect require selecting for a method that will furnish us with the final result of finding hydrocarbon in the porous and permeable rocks (Jerome, 1997). In this respect, well logs have come in a big way to reduce the risk of drilling dry wells. This technique is used to investigate and assess the Lamu basin and in order to produce its accurate interpretation in terms of hydrocarbon potential and to encourage further exploration activities in the basin.

Exploration works have been conducted in the area since 1933 and up to the present time, 16 wells have been drilled many of which were poorly located because they were focusing primarily on Mesozoic objectives, namely; marine Jurassic and Cretaceous rocks that are visible in a few poorly exposed outcrops. Emphasis was also on locating structural accumulations. Knowledge of geological structure alone is no longer adequate to successfully delineate favorable prospects. An understanding of the stratigraphic attributes of the area has therefore been necessary. The basin is under-explored with regard to stratigraphic traps. This is probably because stratigraphic traps are more difficult to identify than traditionally targeted structural traps. Stratigraphic traps do not show an obvious trapping mechanism, as they do not have a "container" closure. Closure is provided by the impervious rocks that will not let oil or gas to pass through it.

Lamu basin is still under-explored in terms of stratigraphic traps. It is no secret that the largest oil fields in the USA are stratigraphic. For instance East Texas field is the largest stratigraphic trap accumulation ever found, (Schlumberger, 1989). Giant Aneth field of Southeastern Utah (controlled by porosity and permeability changes in carbonate reservoir rock) and Southern Florida carbonate rocks production from reefs and traps caused by permeability and porosity variances are other examples (Schlumberger, 1989).

4

The task of evaluating reservoir properties and detecting stratigraphic details was successfully attempted in the Lamu prospect using electric logs. The results obtained are discussed in this dissertation.

1.2 Study area

1.2.1 Location

The study area is situated in South eastern Kenya, on longitude between 39^0 E and 42^0 E and the latitude between 1.00^0 N and 5.00^0S (Figure 1). The Lamu basin covers both the coastal onshore and offshore areas with an aerial extent of 132,720 sq km and sediments thickness ranging from 3 km (onshore) to 13 km (offshore).

1.2.2 Physiography and Geomorphology

Three physiographic zones are observed on the Kenya coast. Nyika lies at 600 metres above present sea level and represents the higher ground covered by the Duruma series and older rocks to the west. Nyika is a well preserved remnant of an end of Tertiary erosion surface (Schulter, 1997). The foot plateau occurs at an elevation of 140 metres. On average, this belt increases in width from a few kilometres in the southern sector, to over 40 kilometres in the north.

The geomorphology is dominated by a series of raised old sea level terraces and the modern shore configuration follows the 0-5 metres and 5-15 metres sea level terrace complexes. The region is generally low lying and characterized by an extensive fossil reef which lies a few meters above the present sea level. It is backed in the interior by a line of hills that rarely exceed 300 metres except in southern parts where Shimba Hills reach an altitude of about 1000 metres above sea level (UNEP, 1998).
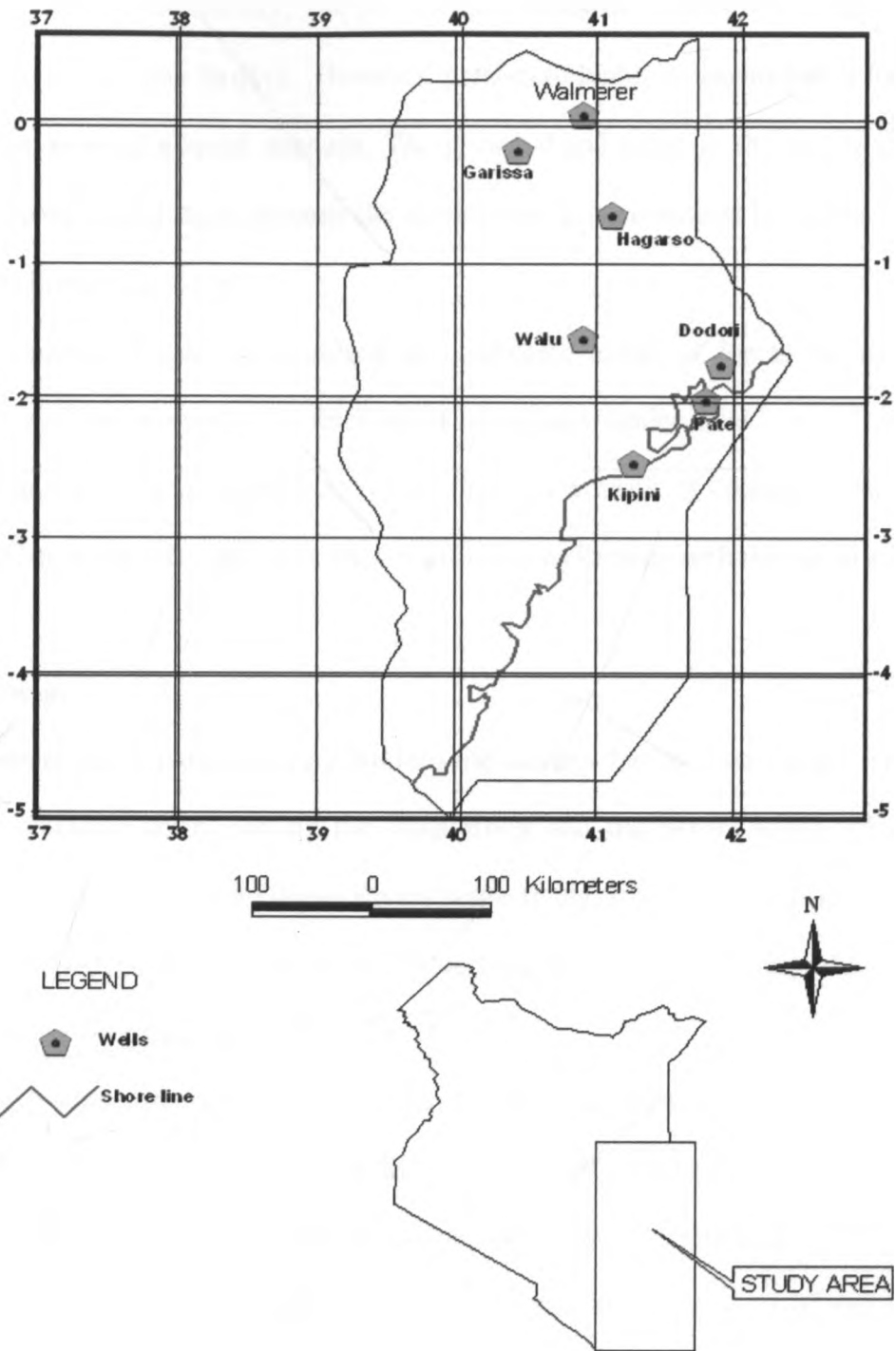
Figure 1.0: Map showing the location of the study area

1.2.3 Soils

Soils show considerable variety. The porous parent rock of sedimentary origin generally gives rise to soils of low fertility. However, patches of highly productive soils have been observed in areas of alluvial deposits. The principal soil types in the region include a narrow strip of coastal sands towards the north where it is permeated by narrow bands of grumusolis brown clay soils.

The soil south of Lamu is composed of bi-attenate bands of loams beyond which grumusolis soils are permeated by thick bands of ash and pumice soils.

The shoreline in most of the region is receding. As a result of coastal erosion, sands supplied from rivers and coral reefs are not sufficient to keep up with the rise in sea level.

1.2.4 Drainage

Both perennial and seasonal rivers drain into the western Indian Ocean basin. There are two main perennial rivers namely the Tana River and the Sabaki River, which also incorporates the Athi and the Galana Rivers respectively. Each of these perennial rivers has catchment extending far from coastal hinterland into the high country of Mt. Kenya region and the Aberdare range in central Kenya.

Tana River is approximately 850 kilometres in length and it has a catchment of 95,000 square kilometres and is replenished by a number of tributaries which have their headwaters on Mt. Kenya. In terms of annual freshwater and sediment discharge, the Tana River has the greatest volume of fresh water and highest amount of sediment. It discharges an average of 3 million tonnes of sediment per year (UNEP, 1998). It enters the ocean about half way between Malindi and Lamu, near Kipini, into Ungwana

(Formosa) Bay. It gives off a branch, which leads to the complex of tidal creeks, flood plains, coastal lakes and mangrove swamps known as the Tana Delta. The delta covers some 1300 square kilometres behind a 50 metres high sand dune system, which protects it from Open Ocean in Ungwana Bay.

There are also a number of lakes with a greater number being found in the Tana Delta. Most of these lakes are quite small and shallow and are typical oxbow lakes, remnants of various meanders of the Tana River Examples of such lakes are Bisila and Shakakobo.

Figure 1.1: Sand dunes at Tana River mouth (UNEP, 1998)

1.2.5 Climate

The area lies in the hot tropical region where the weather is influenced by the great monsoon winds of Indian Ocean. Climate and weather systems on the Kenyan coast are dominated by the large-scale pressure systems of the western Indian Ocean and the two distinct monsoon periods (UNEP, 1998).

From November/December to early March, the weather is dominated by NE monsoon, which is comparatively dry. During March and April, the wind blows in an easterly to southeasterly direction with strong incursions of maritime air from Indian Ocean bringing heavy rains.

During the months of May, June, July and August, the southeasterly monsoon influence gradually sets in and the weather becomes more stable with dull and comparatively cooler temperatures. Between September and November, the NE monsoon gradually re-establishes itself and by December the northern influence is dominant once again.

1.2.6 Rainfall

A relatively wet belt extends along the entire Indian Ocean coast of Africa and its annual rainfall on the Kenyan coast follows the strong seasonal pattern outlined above. The main rains come between late March and early June with the rainfall decreasing from August. Some rains occur between October and November but from December, rainfall decreases rapidly once again to a minimum during January and February (UNEP, 1998).

Mean annual total rainfall ranges from 508 mm in the drier, northern hinterland to over 1,016 mm in the wetter areas south of Malindi.

Relative humidity is comparatively high all the year round, reaching its peak during the wet months of April/July. Evaporation increases from July to March.

1.2.7   Wind

The windiest time of the year at the Kenya coast is during the SE monsoon from May to September, while the calmest months are March and November when the winds are also more variable in direction (UNEP, 1998).

Wind records from Lamu, Malindi and Mombasa shows a consistent daily pattern whereby wind strength (in knots) drops during the night and is always less at 0600 hours than at 1200 hours. This pattern is less pronounced in Lamu, which also tends to be the windiest place on the coast at 0600 hours.

1.2.8   Geology

The Lamu basin environments are set in a passive continental margin, the evolution of which was initiated by the break-up of the mega continent Gondwanaland in the lower

10

Mesozoic. The initial opening up of the Indian Ocean was preceded by doming, extensive faulting and downwarping similar to that observed in the modern Great Rift Valley of Eastern Africa. These tectonic movements formed a N-S trending depositional basin. During the Mesozoic, the resulting graben was exposed to numerous marine incursions and by Jurassic, purely marine conditions are thought to have existed. Tethyan Sea invasion dominated the Middle-Jurassic basin fills. Ceasation of the relative motion between Madagascar and Africa in the Early Cretaceous heralded the passive margin development and deltaic sediment progradation until Paleogene (Nyagah et al., 1996). Prior to rifting, the Lamu basin was located adjacent to Madagascar (Coffin and Rabinowitz, 1988). Shallow seas transgressed the basin in the Miocene when another carbonate regime prevailed.

1.2.9 Stratigraphy

Understanding the stratigraphy of a particular basin is the first step in deciphering its internal relationships and geologic history. It leads to an understanding of the geometry of individual units and their depositional environments.

Deposition occurred in variable, shallow marine environment, providing dense, micritic limestones interbedded with dark grey –brown shales and fine grained sandstones. These sediments wedge out in shallower parts of the Lamu embayment to the North and to the South. Deposition probably took place in a fluvio-littoral, deltaic environment with constantly changing shorelines, (Walter and Linton, 1972).

Periodic Marine incursions produced thin limestone beds while occasional onset of swampy conditions led to the deposition of alluvial silts and lignite. To the North and

11

West, the marine influence disappears entirely resulting in unfossiliferous sequence. Throughout the Tertiary, the basin experienced further faulting and continental erosion. The older Cretaceous deposits were totally removed in many areas. The present day configuration, however, evolved during Pleistocene to the Recent times, a period marked by numerous fluctuations in sea level.

According to Nock, (1999), the stratigraphy of Lamu basin is divided into four Megasequences (Karoo-Jurassic, Cretaceous-Early Paleocene, Paleocene-Eocene, Miocene-Recent) separated by regional unconformities. The unconformities are related to a series of tectonic pulses that resulted in the development of new structures and periods of increased subsidence.

1. Megasequence I (Karroo Group and Jurassic)

They include strata that range in age from Permo-Carboniferous to Early Jurassic. They comprise in ascending order Taru grits, Maji ya Chumvi beds, Mariakani and Mazeras sandstones.

2. Megasequence II (Sabaki Group)

These comprise the entire sequence of rock units between the Late Jurassic and the Late Paleocene unconformity. They include the products of the two marine regressions and intervening transgressions that were deposited in tide-influenced shelf and marine settings, in ascending order these are Ewaso Sands, Walu Shale, Hagarso Limestone, the Freretown Limestone and Kofia Sands.

3. Megasequence III (Tana Group)

This includes the strata that were deposited in fluvial, deltaic and restricted-shelf. They range in age from Paleogene (Eocene to Oligocene). Lithostratigraphic units in this Group include the Kipini Formation. The alternating deposition of shelf carbonate facies and siliciclastic sediments of the Kipini formations associated with the pattern of episodic uplift and subsidence prevailing during the Paleogene.

4. Megasequence IV (Coastal Group)

At the onset of Megasequence IV sedimentation, rejuvenation of the Walu Kipini high and reactivation of faults in Tana syncline took place. Lithostratigraphic units in this Group include the Baratumu formation which constitutes an upward –shoaling inner shelf facies also deposited during periods of subsidence and sea level fluctuations. Reefal build-ups in the middle to outer shelf and shelf edge settings and shales in deeper parts of the basin also took place. Lamu Reefs, Shimba shales and the overlying Marafa Formation, represent these. The figure below illustrates the Lamu basin stratigraphy.

1.3   Previous Work

Various workers have noted the petroleum potential of Lamu basin. Simiyu,(1989) studied the stratigraphic and structural configuration of the basin. His findings were that the potential of sediments as oil progenators in the basin increases with depth towards the sea and that the area has a number of structural highs that could form good traps. Deltas are examples of depositional regressions, for they result from the volume of sediments supplied by river exceeding the volume that can be removed by the sea, (Richard, 1973). These tend to accumulate porous and permeable rocks, which are potential petroleum reservoir rocks.

Large petroleum accumulations tend to occur in reservoir rocks located close to the center of generative basin or on structural highs neighboring deeper generative depressions. Large volumes of hydrocarbon generating sediments and long time spans for drainage are prerequisites for giant oil and gas accumulations, (Gerhard, 1992). Lamu embayment is categorized as an epicratonic embayment. Most of producible hydrocarbon and largest oil fields in the world occur within range of generative depressions. These conclusions apply to the different types of basins for example intracratonic, rift basins, and passive margins, (Gerhard, 1992).

Selly, (1985) has noted embayments as the most productive sedimentary basins for petroleum, much more than intracratonic basins. Not only do they contain marine sediments and better source potential (hydrocarbon source rocks may be defined as fine grained sedimentary rocks which in their natural settings have generated, are generating, or will generate and release enough hydrocarbon to form a considerable accumulation of oil and gas) (Brooks and Fleet, 1987) but, they occur where the continental crust is

15

thinning and less stable, thus heat flow is high and this favour hydrocarbon generation and maturation. Source rocks reach thermal maturity after a relatively short time span and can generate hydrocarbons. Crustal instability also favours structural entrapment (North, 1984)

A thick sequence of sedimentary rocks are estimated to reach a maximum depth of 1,500metres in some areas accumulated along the continental margin in a geosyncline setting that preceded the opening up of Indian Ocean. The sediment sequence varies from Recent to Triassic. However, good source rocks are anticipated at a depth of 3,000-4, 000 metres in the Tertiary-Cretaceous sequence (Caswell, 1956).

The Tertiary deposits have been penetrated by many wells, but the Cretaceous has only been penetrated in few places. The Cretaceous occurs at a depth of 3450 metres in the Lamu and, therefore good mature source rocks are anticipated. Studies have revealed good source rocks, reservoir rocks for hydrocarbon deposits in the basin and the possibility of hydrocarbon reserves exists, (UNEP, 1998).

Prospecting activity in the Lamu basin started way back in 1933, when Anglo-Saxony Petroleum Company and Darcy Exploration Company were awarded an exploration license. Failure to strike oil was attributed to the area being highly faulted, hence opportunity for seepage. During 1959, four wells were drilled by B.P. Shell with an aim of establishing the Stratigraphy. This revealed Pliocene succession of calcareous sands with marine fossils, Miocene limestone with interbedded shales and minor calcareous sands showing cyclic sedimentation

Between 1954 and 1971, Shell and British Petroleum (BP) conducted seismic surveys, which were used to delineate a number of seismic highs on which deep wells were

drilled. The efforts were invigorated in 1970s by both independent and transnational prospectors following a surge in oil prices. During 1926.67, Shell-Esso drilled three wells

In 2004, National Oil Corporation of Kenya (NOCK) signed production-sharing agreements with two major oil companies. These are Dana Petroleum and Woodside, a consortium from Australia and Afrex and Pan Continental.

1.4 Statement of the Problem

The prices of fossil fuels continue to sky rocket each day. This is basically because the demand for the commodity does not match its supply. This has a far reaching consequence especially on the countries and Kenya, being one of them that does not produce the commodity has to depend on importing to meet its domestic and industrial uses.

World oil demand is conservatively expected to increase from the current 76 million barrels per day against the 66 million barrels that is being produced daily. What this means in real terms is that if the very conservative figure of 4% growth per year is used, world oil supplies will have to double. We are consuming many of our resources more rapidly than we can discover new sources.

The proven worldwide oil reserves are estimated at about 350 billion barrels already located underground. This would only be enough to last not more than 30 years at the present rate of consumption, and then the inevitable conclusions are that the demand will always be on the rise, prices will sky-rocket and eventually reserves will be depleted.

17

Hence, this calls for stepping up prospect work in the sedimentary basins that have shown indication of striking these fossil fuels. Lamu basin is a prospect hydrocarbon basin and in order to fully exploit its potential, there is a dire need to explore it using the method of geophysical well logs to locate areas that are likely to contain stratigraphic types of oil and gas traps. Electric logs are used to quantitatively estimate the reservoir parameters of porosity. In addition, lithologic data is applied to construct fence diagram which is instrumental in demonstrating the changes in lithofacies, pinchouts, truncations and other stratigraphic relationships that form oil and gas traps occurring in the region. Previous studies done in the Lamu basin have been directed towards identifying structural types of traps but none on stratigraphic types

1.5 Justification

Fossil fuels continue to be the main driving force in all sectors that depend on this type of commodity be it industrial or domestic use. With the increase in demand for oil, there is need for the country to have its own source of energy and this can only be achieved by stepping up prospecting in the potential basins of which Lamu basin is one of them. This will only be accomplished by adopting the technique of geophysical well logs. With this technique, evaluation of reservoir parameter will be achieved and this will necessitate exploration for the stratigraphic types of traps in the Lamu basin that have in the past received little or no attention from the past studies.

While Lamu basin stratigraphic traps may be under-explored and under-utilized, it is no secret that the largest oil fields in the USA are stratigraphic (Schlumberger, 1989). To fully exploit these potential reserves, there is need to apply geophysical well log data to

18

evaluate the subsurface reservoir fluids and in detecting stratigraphic details that would pinpoint to stratigraphic traps.

1.6 Significance

The project has come at a most appropriate moment when the prospect of oil and gas is raising great expectations in everyone's mind and the thoughts are being directed to the future pattern of the energy industries of Kenya and to the vital role of energy in the economic direction. The potential impact of discovering oil and gas on the energy industries will no doubt strengthen the economy.

It seems inescapable therefore that we must find and use our own oil supplies where we can stabilize expanding population and technological advances. We are at risk of large fluctuations in the balance between our import account and export earnings and especially if oil prices are very volatile that adversely impact national budgets.

In general, nothing will underrate the benefits that are associated with a country being energy independent. Social and economic impacts will be immeasurable.

1.7 Aim and Objectives

1.7.1   Aim

To explore the Lamu basin with regard to targeting stratigraphic traps

1.7.2   Specific Objectives

❑   To identify formations of interest and to evaluate reservoir parameters,

❑   To achieve well-to-well stratigraphic correlation;

❑   To identify approximate area of major pinch out and unconformities;

❑   To predict the zones where the stratigraphic traps ought to be.

2.0 Fundamentals of Geophysical Well Logs

The conventional electrical survey usually consists of a Spontaneous Potential (SP), 16-inch Normal, and 64-inch Normal, and 18-feet 8-inch lateral devices (see Figure 2.0 below). The currents are passed through the formation via certain electrodes (Schlumberger, 1989) and voltages are measured between certain others. This measured voltage provides the resistivity determination for each device so that there will be a current path between electrodes and the formation. The sonde must be run in holes containing electrically conductive mud or water.
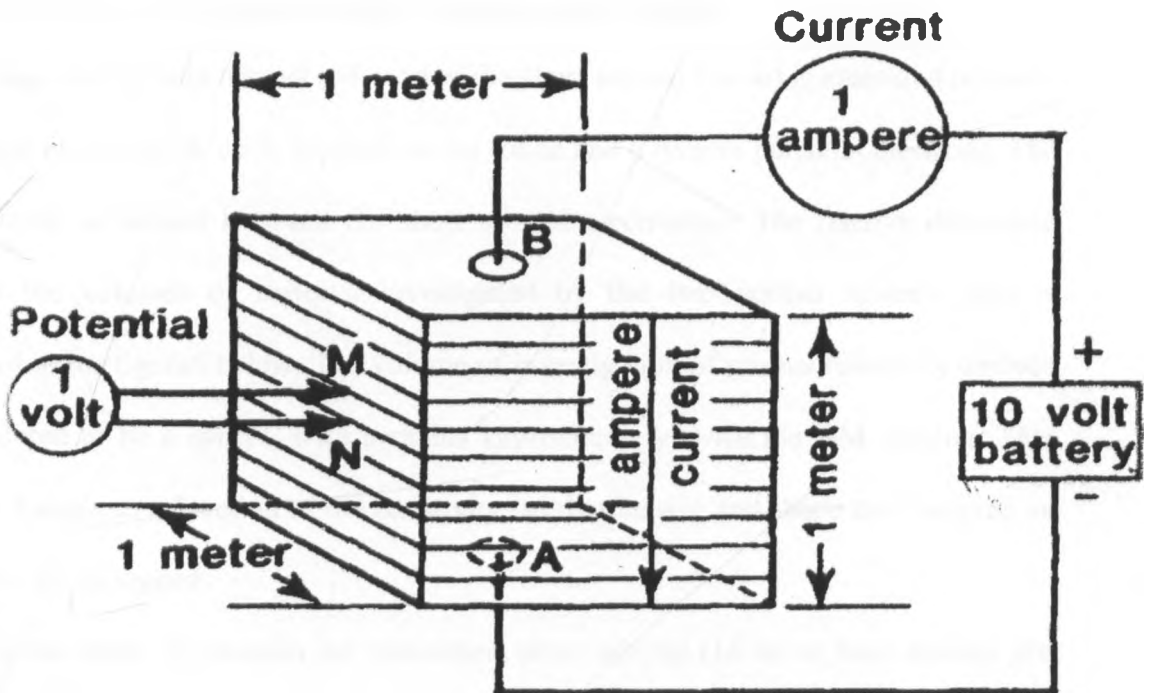
Figure 2.0: Set up for measuring resistivity in ohm metres

The current is passed between electrode A and B and the voltage drop is measured between potential electrodes M and N. For normal resistivity logging, electrodes A and M are located well relatively close together, and electrodes B and N are distant from AM

and from each other. Electrode configuration may differ in equipment produced by different manufacturers.

The electrode spacing, from which the normal curves derive their name, is the distance between A and M, and the depth reference is at the midpoint of this distance. The most common AM spacing are 16 and 64-inch; however, some loggers have other spacing available, such as 4, 8, 16 and 32 in. The distance to the B electrode which is usually on the cable, is approximately 15m, is separated from the AM by the insulated section of cable. The N electrode usually is located at the surface, but in some equipment, the locations of B and N may be reversed. Constant current is maintained between an electrode at the bottom of the sonde and remote-current electrode.

The voltage for the long normal (64-in) and the short normal (16-in) is measured between a potential electrode for each, located on the sonde and a remote potential electrode. The SP electrode is located between the short normal electrodes. The relative difference between the volumes of material investigated by the two normal systems also is illustrated in the figure5 below. The volume of investigation of normal resistivity devices is considered to be a sphere, with a radius approximately twice the AM spacing. This volume changes as a function of the resistivity, so that its size and shape are changing as the well is being logged.

As far as the depth of invasion are concerned, short normal (16 in. or less) devices are considered to investigate only the invaded zone, and long normal (64-in) devices are considered to investigate both the invaded zone and the zone where native water is found. Long response is affected significantly by bed thickness, this problem can make the logs quite difficult to interpret. The bed-thickness effect is a function of electrode spacing.

Normal logs measure apparent resistivity; if true resistivity is to be obtained from these logs they must be corrected with the appropriate Schlumberger charts.
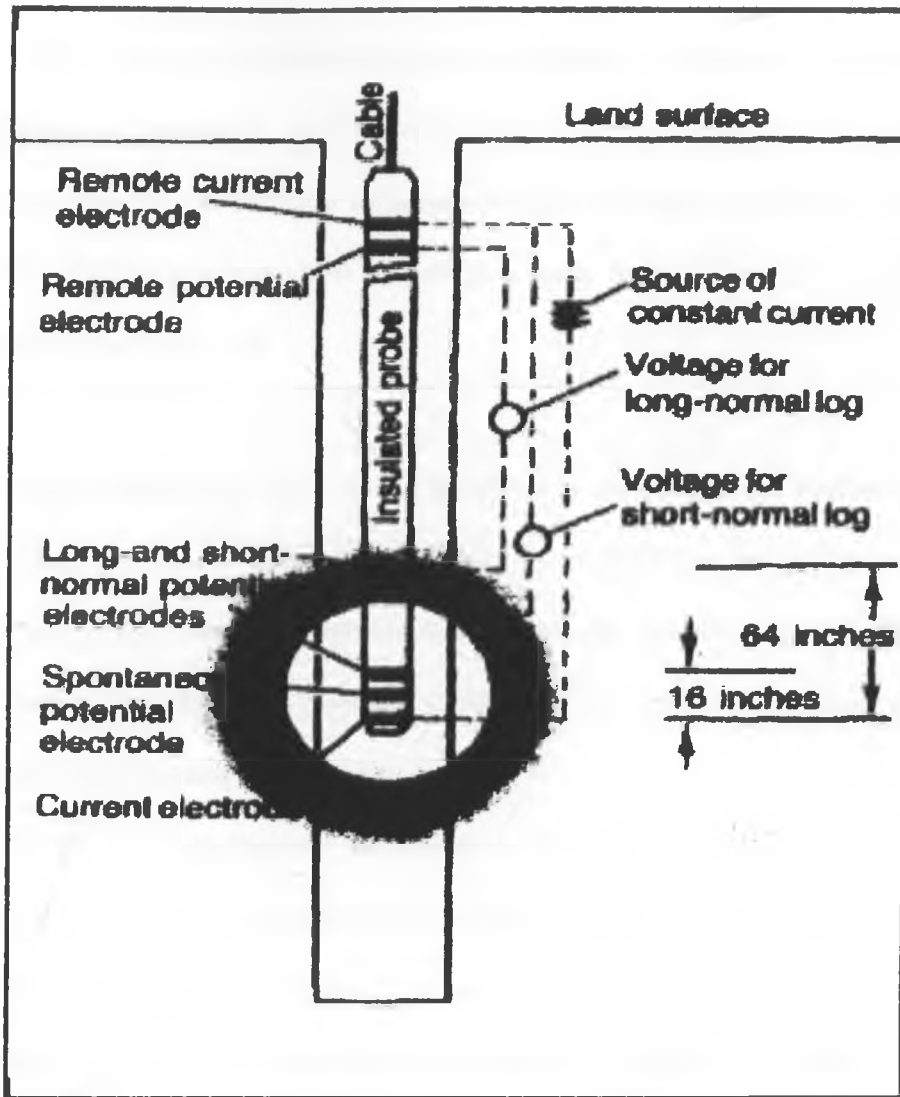
Figure 2.1: Systems used to make 16- and 64-in. normal resistivity logs. Shaded areas indicate relative size of volumes of investigation.

Courtesy, Schlumberger Well Services. Copyright 1977, Schlumberger.

2.1 Reservoir Parameters Evaluation

Almost all oil and gas produced today come from accumulation in pore space of reservoir. The amount of oil or gas contained in unit volume of a reservoir rock is the product of its porosity by hydrocarbon saturation. Porosity is defined as the pore volume per unit volume of formation. Hydrocarbon saturation is the fraction of pore volume filled with hydrocarbon. In addition to porosity and hydrocarbon saturation, the volume of formation containing hydrocarbon is needed in order to determine if an accumulation is to be considered commercial.

To evaluate producibility of a reservoir formation, it is useful to know how easily a fluid can flow through the pore system. This porosity of a formation, which depends on the manner in which the pores are interconnected, is its permeability. The main physical parameters needed to evaluate a reservoir then are its porosity, hydrocarbon saturation, permeable bed thickness and permeability.

These parameters are inferred or derived from electrical logs. This dissertation is concerned mainly with the determination of reservoir porosity, hydrocarbon saturation and resistivity. Of parameters obtained directly from logs, resistivity is of particular importance and it is essential to hydrocarbon saturation determination, hence, it will also be determined. Resistivity measurements are used, singly and in combination to deduce formation resistivity in uninvaded formation, i.e., beyond the zone contaminated by borehole fluids, where mud filtrate has largely replaced original fluids.

2.2 Resistivity Determination

The resistivity of a substance is its ability to impede the flow of electric current through that substance. The resistivity units used in electrical well logging are ohm-metre^2/metre, usually written ohm-m. The resistivity of a formation in ohm-metres is the resistance in ohms of one-metre cube when the current flows between opposite faces of a cube. Electrical conductivity is the reciprocal of electrical resistivity and is expressed in mhos per meter. In electrical well logging practice, conductivity is expressed in millimhos per metre (mmhos/m). The resistivity of a formation is the key parameter in determining hydrocarbon saturation. Electricity can pass through a formation only because of the conductive water it contains, with a few rare exceptions such as metallic sulfide and graphite; dry rock is a good electrical insulator. Therefore, the subsurface formations have finite, measurable resistivities because of the water in their interstitial clay. The resistivity of a formation depends on:

➤ Resistivity of formation water;

➤ Amount of water present;

➤ Pore structure geometry;

The resistivity (specific resistance) of a substance is the resistance measured between opposite faces of a cube of that substance at a specified temperature. The metre is the unit of length and ohm is the unit of electrical resistance. In abbreviated form, the resistivity is;

$$R = \gamma A / L \ldots\ldots\ldots\ldots\ldots\ldots\ldots\ldots\ldots\ldots\ldots\ldots\ldots 2.0$$

Where, **R** = Resistivity in ohm-meters

24

γ = Resistance in Ohms

A = Area in square metres

L = Length in metres

2.3 Spontaneous Potential Log Curve

These are recordings of naturally occurring physical phenomena in in-situ rocks. SP log curve is record of direct current (DC) verse voltage differences between the naturally occurring potential of movable electrode in the borehole and the electrical potential of fixed surface electrode, (Schlumberger,1989). The electrical potential (voltage) is produced or develops at the contacts between shale or clay beds and sand where they are penetrated by a drill hole.

The chief sources of spontaneous potential in a drill hole are electrochemical or streaming potentials and redox effects (Asquith, 1982). Streaming potentials are caused by the movement of electrolyte through permeable media. These permeable intervals frequently are indicated by rapid oscillations on an otherwise smooth curve.

The SP curve usually defines a more-or-less straight line on the log, called the shale baseline. Opposite permeable formations, the curve shows excursions (deflections) from the shale baseline, in thick beds, these excursions tend to reach an essentially constant deflection defining a sand line. The deflection may be either to the left (negative) or to the right (positive) depending primarily on the relative salinities of the formation waters and of the mud filtrate. SP log is recorded in millivolts (mV) per unit of chart paper or full scale on the recorder (Asquith, 1990).

25

Lithologic contacts are located on SP logs at the point of log inflection, where current density is maximum. When the response is typical, a line can be drawn through negative values that represent intervals of clean sand. The maximum positive SP deflections represent intervals of fine-grained material, mostly clay and silt; the maximum negative SP deflections represent coarser sediments. SP logs have been used widely for determining formation-water resistivity (R_w) in oil wells. The SP deflection is read from a log at a thick sand bed; Rm is measured with a mud-cell or fluid conductivity log. Temperature may be obtained from a log, but it can also be estimated, particularly if bottom-hole temperature is available.

2.4 Saturation

The term saturation refers to the percentage of the rock pore space that is filled with each of the three fluids; oil, gas or water. The total of the three will always be 100 percent as there is no such a thing as empty porosity. It is generally assumed that unless otherwise known, the pore volume not filled with water is filled with hydrocarbon. Determination of water and hydrocarbon saturation is one of the basic objectives of well logging in petroleum industry. All water saturation determinations from resistivity logs in clean formations (nonshaly) with homogeneous intergranular porosity are based on Archie equations or variation thereof.

2.5 Archie Computational Equations

A practical method is based on establishing field-formation resistivity factors (F) using electric logs. After a consistent formation factor is established, the normal curve, or any other resistivity log that provides a reasonably correct R_t can be used to calculate R_w from the relationship: $F = R_o / R_w$ Under these conditions, R_o the resistivity of a rock 100

percent saturated with water, is assumed to approximate R_t after the appropriate corrections have been made. Resistivity from logs can be converted to standard temperature using Schlumberger chart, (Fig. 3.0).

The formation resistivity factor (F) also defines the relation between porosity and resistivity as follows:

$$F = a/\emptyset^m = R_o/R_w, \dots\dots\dots\dots\dots\dots\dots\dots\dots\dots\dots\dots\text{2.1}$$

where, m is the cementation exponent (Archie's formula)

Archie equation remains the keystone of log analysis for the solution of water saturation of potential oil and gas zones:

$$S_w = \left(\frac{a}{\Phi^m} * \frac{R_w}{R_t} \right)^{\frac{1}{n}} \dots\dots\dots\dots\dots\dots\dots\dots\dots\dots\text{2.2}$$

Together with Schlumberger charts; they were invaluable in determining and evaluating reservoir parameters. The equation is actually made up of two separate equations. The first describes the relationship of the ratio of the resistivity of a water-saturated rock, R_o, to its formation water resistivity, R_w, to the fractional porosity, Φ:

$$\frac{R_o}{R_w} = \frac{a}{\Phi^m} \dots\dots\dots\dots\dots\dots\dots\dots\dots\dots\text{2.3}$$

This resistivity ratio is also known as the "formation factor", F. The second equation relates the ratio of the observed formation resistivity, R_t, to its expected resistivity, R_o, if it was completely saturated with water, to the fractional water saturation, S_w:

27

$$\frac{R_t}{R_o} = \frac{1}{S_w^n}$$ 2.4

The equations are universally applied to reservoir fluid calculations from wireline logs in "clean" (shale-free) formations

The application of the Archie equations presupposes knowledge of the parameters, or at least reasonable estimates of them, in order to calculate acceptable water saturation. Formation water resistivity can usually be established from field measurements and/or log analysis estimations. However, the quantities of a, m (the "cementation factor"), and n (the saturation exponent) are usually unknown and their values are given as a matter of experience. The range of values for m and their relationship with rock texture has been the subject of much measurement and discussion. By contrast, the variability of n is less well understood, but is generally taken to be the number 2 (at least, in water-wet zones). The problem is further compounded by the realization that these "constants" are only likely to remain so in relatively homogeneous reservoirs, where rock texture and pore geometry remain fairly uniform. Their values are affected by tortuosity of the path that electrical current must take while flowing through the pores of the rock. Continuing advances in theory and measurement demonstrates that simple models may be poor (and puzzling) representations, or even downright misleading in heterogeneous and complex reservoirs that are the targets of many of today's energy companies.

2.6 Formation Water Resistivity

Formation water resistivity represents the resistivity value of the water (uncontaminated by drilling mud) that saturates porous formation. It is also referred to as connate or interstitial water. Schlumberger (1989) defined formation water as the water uncontaminated by drilling mud that saturates the formation rock. Its resistivity can be determined by a number of methods. Discussed here in this work is the SP method. Analysis of wireline log data depends on the assumption that the only conductive medium in a formation is the pure water, which supplies the energy and drive in the reservoirs. Hence the properties of these formation waters can be determined, one of which is its electrical resistivity and this eventually leads to water saturation (Sw), an important aspect of reservoir evaluation.

Formation water resistivity is variable depending on the temperature, salinity and whether or not the formation contains hydrocarbons. At a given salinity, the higher the temperature the lower the resistivity and the water resistivity at any formation temperature can be calculated from the water resistivity at another formation temperature, knowing both the temperature offset using the form

$$R_w \text{ at } FT2 = R_w FT1, (FT1+C)(FT2+C) \dots\dots\dots\dots\dots 2.5$$

Where, $FT1$ = Initial formation temperature

$FT2$ = Formation temperature from which R_w is

determined,

$C = 21.5$ for temperature in 0° C (Smolen, 1977).

Temperature, resistivity and formation water resistivity is not only a function of salinity but also a function of temperature. The three variables must be known to uniquely define

a solution. It should be noted that during a well log operation, a maximum reading thermometer is run which measures the bottom hole temperature. To determine the temperature at any other location in the borehole, it is assumed that its geothermal gradient is linear. The relationship between temperature and geothermal gradient is given by:

$$T_f = T_o + GgD_f/100 \dots\dots\dots\dots\dots\dots\dots\dots\dots\dots\dots\dots\dots\dots\dots 2.6$$

where, T_f = Temperature of any formation

T_o = Mean surface temperature

G_g = Geothermal gradient in $^0C/100$ metre

D_f = depth to the formation

The surface temperature is the average of the day-to-day and season-by-season and year-by-year variations

CHAPTER THREE

METHODOLOGY

3.1 Data Acquisition and Analysis

The geophysical well log data had been obtained at the Lamu basin well sites by BP-Shell Oil Company between 1971 and 1975. The data which is in analog form is kept by National Oil Corporation of Kenya in their archives. The type of well log applied in this kind of study is electrical induction log which was available for the seven well locations namely Dodori-1, Kipini-1, Walmerer, Walu-2, Garissa-1, Hagarso –1 and Pate-2.

Desk study was carried out in order to acquire the relevant information that was required to meet the objectives of the project. First was to obtain the information from the log header which contained the data that is required to estimate the reservoir parameters and also from the log curves. In addition, lithology data was acquired to be used in desk study also involved study of reports, Schlumberger charts and figures and books that contained information on how to go about with well logs analysis and interpretation.

3.2 Log analysis

The process, called log analysis, combines the measurements in series of numerical models, thereby converting the raw data into useful information. The output of this interpretation was a detailed numerical analysis of the reservoir rocks, yielding information on formation porosity. The objective was to utilize the available logs to obtain an analysis of the reservoir properties over the stratigraphic horizon considered. The information from the log header (Table 3 0) was utilized in the calculation of resistivity values of fluids that is R_m, R_{mc}, R_{mf} at formation temperature.

Table 3.0: Data table from log header

Well	T_D (m)	Rm (ohm-m)	Rmf (ohm-m)	Rmc (ohm-m)	SP (mv)	Thickness (m)	Tsurf (°C)	BHT (°C)
Pate	4189.17	$0.222@26.67^0$	$0.15@26.67^0$	$0.357@26.67^0$	-8	7.62	26.67	124.44
Garissa-1	1221.64	$0.7@26.67^0$	$0.5@26.67^0$	$1.0@26.67^0$	-10	3.05	26.67	63.33
Kipini	3642.06	$0.16@65.56^0$	$0.09@65.56^0$	$0.5@65.56^0$	-10	3.05	65.56	128.89
Dodori	4287.32	$0.18@32.22^0$	$0.35@32.22^0$	$0.85@32.22^0$	-30	15.24	32.22	146.11
Hagarso	1497.48	$0.89@26.67^0$	$0.68@26.67^0$	$1.05@26.67^0$	-15	10.06	26.67	74.44
Walu	3642.06	$0.16@65.56^0$	$0.09@65.56^0$	$0.5@65.56^0$	-10	3.05	65.56	128.89
Walmerer	3854.50	$0.54@25.56^0$	$0.15@25.56^0$	$1.06@25.56^0$	-14	18.29	25.56	137.25.

These values were later used to arrive at formation water resistivity (R_w) which is an important parameter required in determining the porosity of the formation. Since temperature of formation is important in log analysis, it had to be determined graphically by use of Schlumberger chart and by calculation using linear regression equation. This is because the Resistivities of fluids vary with temperature

The resistivity curves used were induction electric log (Fig 3.1). The log track on the far left track#1 contains SP log. The middle track contains two resistivity curves. One measures shallow resistivity (R_i, 16-normal or short normal electrode represented by the solid line). And the other measures deep resistivity (R_t, an induction log represented by the dotted line). Track #3, the log track on the far right contains a conductivity curve

measured by induction log. The induction log actually measures conductivity, not resistivity, but because conductivity is the reciprocal of resistivity, resistivity can be derived. Various Schlumberger charts were used to make the log analysis achievable.

3.3 Formation Water Resistivity determination from SP log

3.3.1 Illustration from Pate Well

The interval of interest in this well is from 3194.30 to 3200.40 m as seen in the electric log curve (Fig 3.2), referred to as Pate limestone Formation. This formation is characterized by lithology that comprise of alternating cycles of oolitic and nummulitic limestones and dark grey to greenish shales that lowers the reservoir quality of the formation. The data of the clean Pate Limestone formation are used to estimate the values of R_w, R_{mc} and R_m which are found out to be 0.045, 0.13 and 0.081 ohms respectively. These values will be used to estimate porosity value of the formation.

3.3.2 Determination of Temperature of Formation (Tf)

This is important in log analysis and had to be determined because the resistivities of the drilling mud (R_m) and mudfiltrate (R_{mf}) and the formation water vary with temperature. The temperature of formation is determined by knowing the following information which is available on the Pate log header (Appendix 1):

- Formation depth;
- Bottom hole temperature;
- Total depth of the well;
- Surface temperature;

33

3.3.3 Formation Temperature determination using Schlumberger Chart

Reasonable values for the T_f can be determined by using the above data and by assuming a linear geothermal gradient using Fig.3.0

For the Pate well,

Surface temperature=26.67^{0}C

Bottom hole temperature=124.44^{0}C

Total depth of the well=4198.32 metres

Formation depth=3927.96 metres

The procedure adopted is as follows:

Locate the Bottom hole temperature, which is 124.44^{0}C on the 26.67 scale (bottom of the chart, surface temperature=26.67^{0}C)

Follow Bottom hole temperature vertically up until it intersects 4198.32 metres total depth. This intersection defines temperature gradient

Follow temperature gradient line up to 3927.96 metres (from the point where 3927.96 metres intersects the temperature gradient. This gives the temperature of formation as 118.89^{0}C

ESTIMATION OF FORMATION TEMPERATURE

Temperature (Degrees Centigrades)
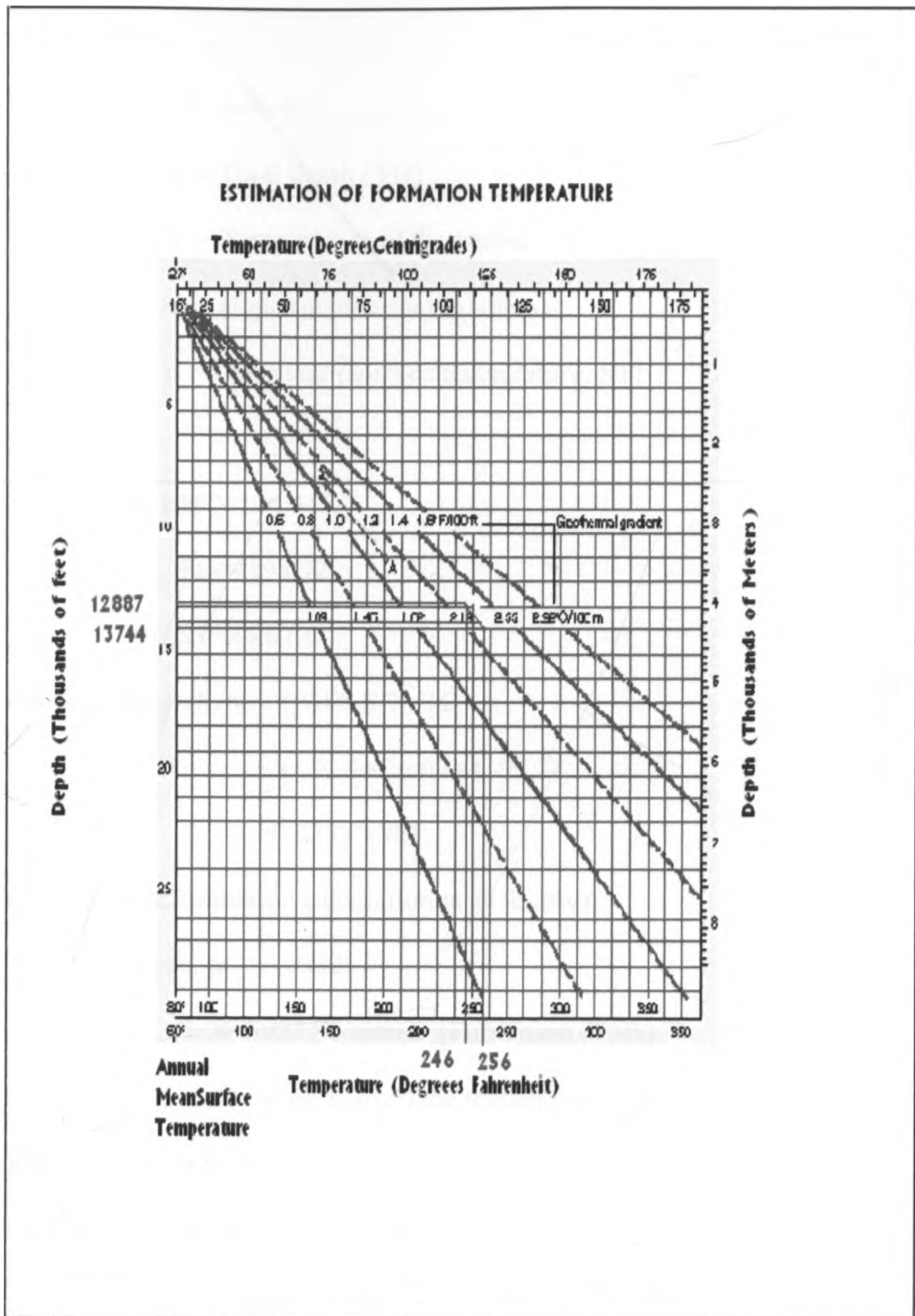
Figure: 3.0 Chart for determination of Temperature of formation. Courtesy, Dresser Industries. Copy right 1975, Dresser Atlas.

Formation temperature is also calculated (Asquith, 1982) by using the linear regression equation:

$$Y = mX+C \dotfill 3.0$$

where,   X = Total depth (TD)

Y = Temperature of formation

m = slope (geothermal gradient)

c = a constant (surface temperature, ST)

Given BHT=124.44^{0}C

TD=4198.32m

ST=26.67^{0}C

Geothermal gradient = (BHT-S.T)/TD

= (124.44-26.67)/4198.32

=0.0232^{0}C/M

Temperature of formation calculation is as follows;

Given, m = 0.0232

X=3927.96 metres (Formation depth)

C=26.67^{0}C (Surface temperature)

Considering that Y=mX+c

hence Y= (0.0232) x (3927.96)+26.67

=119.39^{0}C (temperature of formation at 3927.96 metres).

The value of formation temperature which is found to be 119.39^0C by using the linear regression equation compares well with that derived from the Schlumberger chart which was estimated at 118.89^0C

After the temperature of formation has been determined either by the use of Schlumberger chart or by calculation using linear regression equation, the resistivities of different fluids (R_m, R_{mf}, or R_w) were corrected to formation temperature using Schlumberger chart (figure 3.0), a chart that is used for correcting fluid resistivities to formation temperature (Edwards *et al*, 1963). The chart is closely approximated by Arp's formula

$$R_{Tf} = R_{temp}x(Temp. =6.77)/ (Tf+6.77)\dots\dots\dots\dots\dots\dots\dots\dots\dots\dots\dots3.1$$

Where R_{Tf} = Resistivity at formation temperature

R_{temp} = Resistivity at a temperature other than formation

temperature

Temp = Temperature at which resistivity was measured

T_f= Formation temperature

Given that the resistivities of drilling mud,

$$(R_m) = 0.222@26.67^0F,$$

$$T_f = 119.39^0C,$$

Then, R_m at 246.9 will be,

$$R_m 119.39^0C = 0.222x (26.67+6.77)/ (119.39+6.77)$$

$$=0.069$$

37
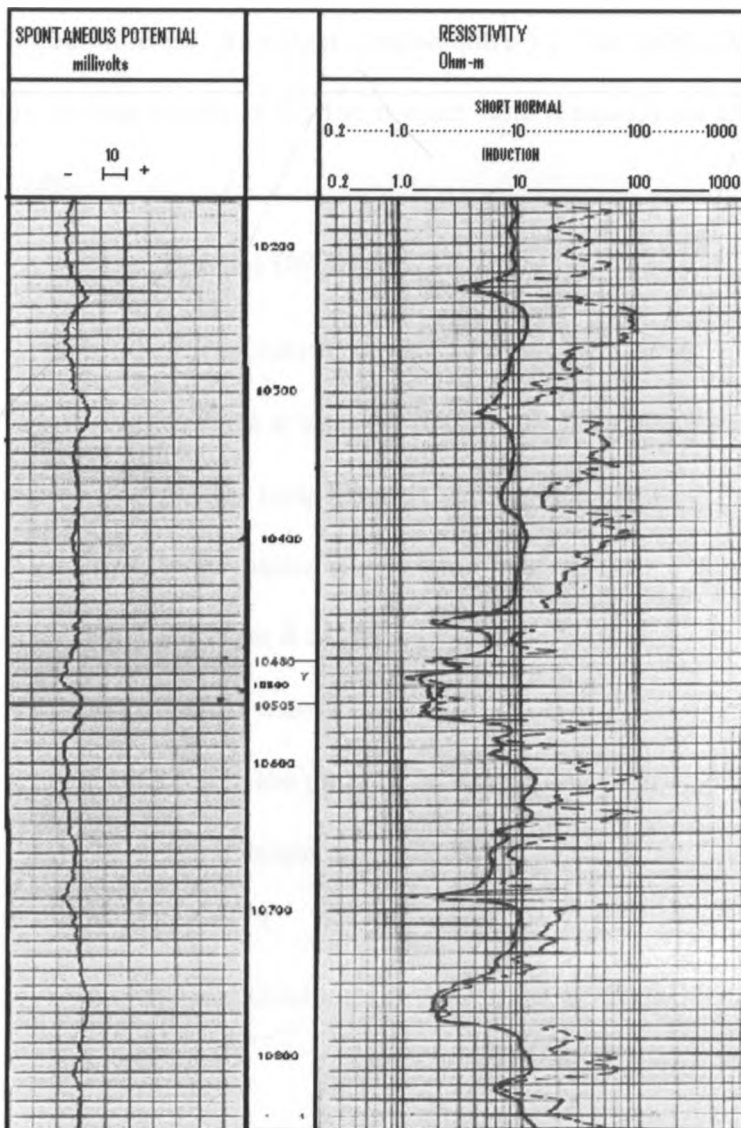
Figure 3.1: Log Data for Pate Well. The letter marked **Y** Represents the Pate Formation

After selecting a particular permeable zone the following procedure below is adopted in determining formation water resistivity, (Parasnis, 1977)

1   Establish the shale baseline on the SP curve.

2.   Pick out clean permeable zones.

3.   Do all the thick zones have about the same SP value? If yes, then pick any thick one, but otherwise, pick thick zone near and/or the zone you are interested in.

4   Determine the formation temperature i.e. the temperature of this zone chosen, using surface temperature, the bottom hole temperature and the total depth with the formula:

$$T_f = (T_{TD} - T_O) \, Df/D_{TD} + T_O \quad \dots\dots\dots\dots\dots\dots\dots\dots\dots\dots\dots\dots\dots\dots\dots\dots\dots\dots\dots\dots\dots\dots\dots \textbf{3.2}$$

Where T_f = Temperature of the formation in °F or °C.

T_{TD} = Temperature at total depth (Bottom hole Temp.) in °F or °C.

T_0 = Mean surface temperature (in °F or °C).

D_f = Depth to formation (in ft or m).

T_D = Total depth (in ft or m).

   $T_D = 3747.21$ metres

   D_F = Depth to the permeable formation = 3200.4

   T_0 = Surface temperature = 26.67° F

   T_{TD} = 124.44° C

   Geothermal Gradient (G. G) = (124.44 - 26.67)/3927.96

                = 0.0249° C/metre

$$T_f = T_0 = + G.G \, D_f \quad \dots\dots\dots\dots\dots\dots\dots\dots\dots\dots\dots\dots\dots\dots\dots\dots\dots\dots\dots\dots\dots\dots\dots\dots \textbf{3.3}$$

$$=26.67+ (3200.4*0.0249)$$

$$=106.33^0C$$

5.   Now, from the R_{mf} and R_m values recorded on the log heading, determine the R_{mf} and R_m values at that particular formation temperature using the formula:

$$R_{mf} \text{ at } T_f = R_{mf} \text{ at } T_0(T_0 + C/Tf +C) \dots\dots\dots\dots\dots\dots\dots\dots\dots\dots\dots\textbf{3.4}$$

Where C is the temperature offset.

$C = 6.77$ if imperial units are used and 21.5 if metric units are used.

T_0 – Initial temperature at which R_{mf} was first measured

R_m – Resistivity of mud, usually recorded on the log heading

From Pate log header, $R_m =0.022$, Rmf, =0.15, $R_{mc}=0.357$

Therefore, using equation 3.3,

    R_{mf} at $T_f=0.15*(26.67+6.77)/ (110+6.77)$

        $=0.0429$

    R_m at $T_f =0.222*(26.67+6.77)/ (110+6.77)$

        $=0.0635$

    R_{mc} at $T_f=0.357*(26.67+6.77)/ (110+6.77)$

        $=0.1022$

From the log track

6.   (i) Now read off SP amplitude (Figure 3.1) from shale baseline to the maximum constant deflection. The value is -8mv

(ii) Determine the bed thickness from SP deflection points. Here the bed thickness is established to be 7.62 metres i.e. (3201.924 to 3194.304 metres)

(iii)Resistivity short normal (R_i) equals 12 ohm-meters

7. Correct SP to SSP. Correcting SP for thin-bed effect will give a value for SSP (Pirson, 1963, Frick 1962).This is achieved with the use of Schlumberger SP correction chart, (figure 3.2).

Given R_i /R_m=12/0.026.67=65.56. Bed thickness read from SP Log (Figure 3.1) equals 7.62 metres. Correction factor (figure 3.2 below) =1.07

SSP=SP X SP Correction factor

SSP= (-8mv) X 1.07

SSP=-8.56
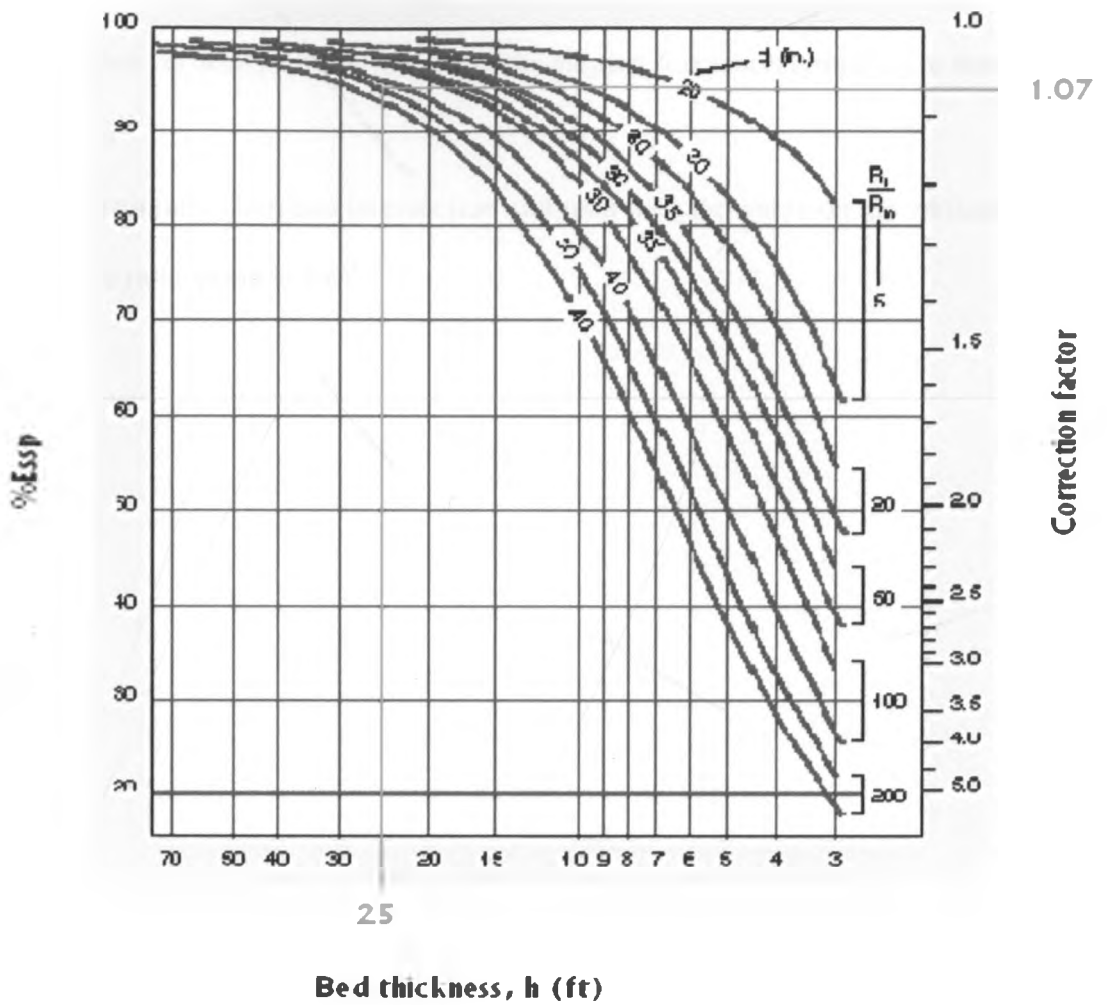
Figure: SP Correction Chart

Figure 3.2: SP Correction chart. Courtesy, Dresser Industries. Copy right 1975, Dresser Atlas.

8 Determination of R_{mf}/R_{we} ratio from SSP values using (figure 3 3)

The procedure is as follows;

(i) Locate an SSP value on horizontal scale (in this case -8.56)

(ii) Follow the value vertically until it intersects the sloping formation temperature line

(119.39^{0}C)

(iii) Follow it horizontally from this intersection and read the ratio value on the vertical

scale   (the ratio value is 1.6)
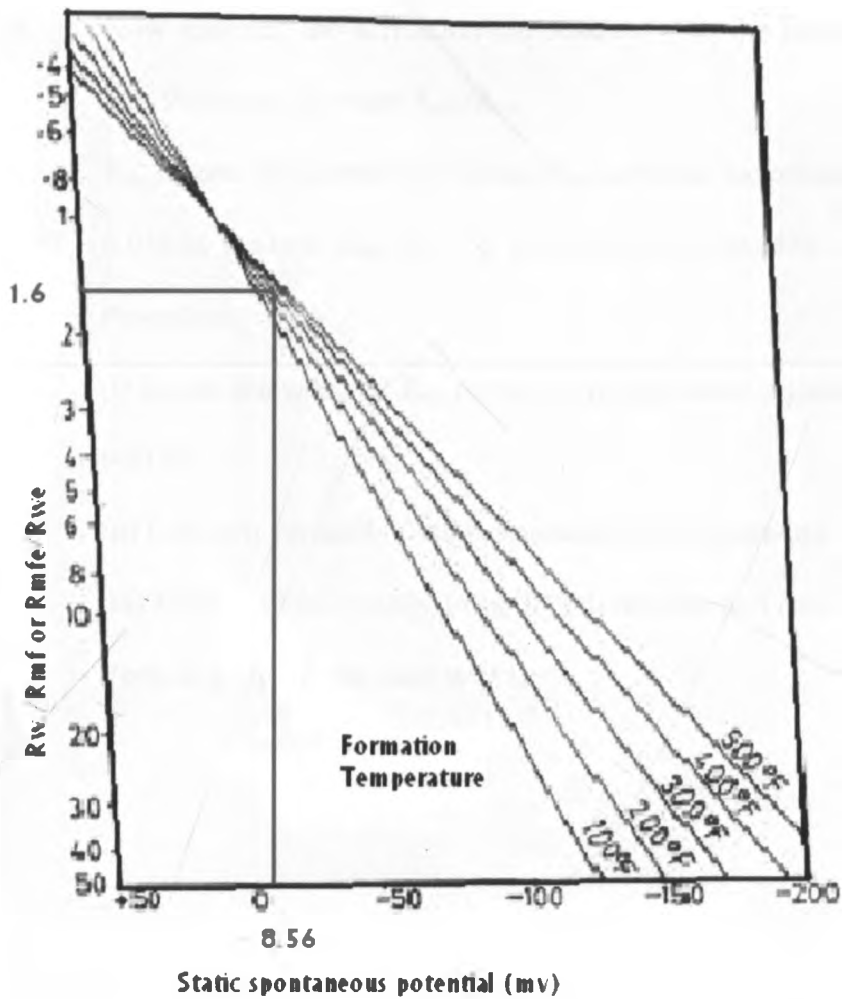
Figure 3.3: Chart for R_{we} determination from Essp. Courtesy, Dresser Industries. Copy right 1975, Dresser Atlas.

3.3.4 Determining Formation Resistivity value, R_w from R_{we}

9. Now knowing the formation temperature (T_f), the static SP or SSP transformed into the resistivity ratio R_{mf}/R_{we}

R_{we} is then calculated by dividing R_{mf} corrected to formation temperature (T_f) i.e. 0.055 by the ratio R_{mf}/R_{we} i.e. (1.6)=0.055/1.6=0.0344

Procedure:

(i) Locate the value of R_{we} on the horizontal scale (figure 3.4). In this case it is 0.0344

(ii) Follow it vertically until it intersects the temperature curve (119.39^0C)

(iii) Follow it horizontally from the intersection and read a value for R_w on the Vertical scale (in this case 0.038)
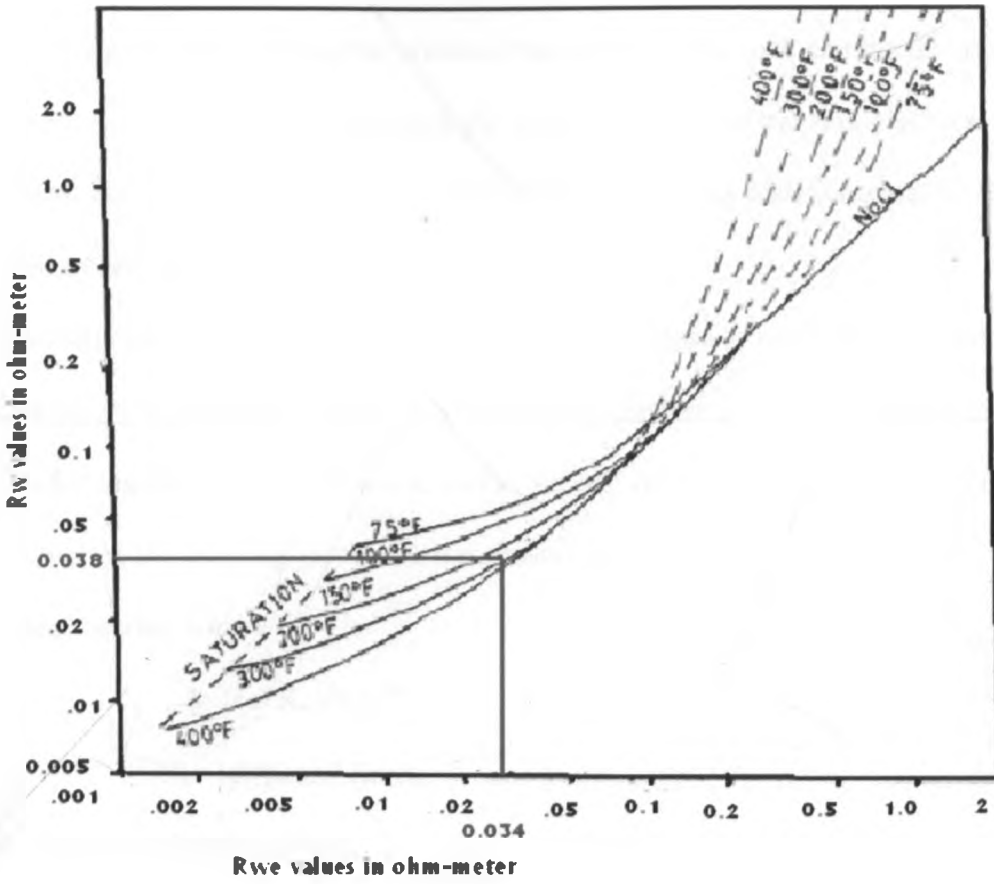
Chart for determining resistivity value for Rw from Rwe

Figure 3.4: Chart for determining R_w from R_{we} Courtesy, Dresser industries. Copy right 1975, Dresser Atlas.

3.4 Resistivity Porosity Determination

The minerals that make up the grains in the matrix of the rock and the hydrocarbon in the pores are nonconductive. Therefore the ability of a rock to transmit electrical currents is almost entirely the result of water in the pore space. Thus resistivity measurements can used to determine porosity.

Normally measurements of a formation resistivity close to borehole, (flushed zone, R_{xo}, or invaded, R_i) are used. In this study, shallow resistivity devices such as short normal of electric log were used to obtain R_i and R_t values. Archie equations below were applied in estimating the porosity values for the considered wells.

Water bearing zone:

$$\phi = \{(a*R_w)/R_t\}^{1/m} \quad\quad\quad\quad\quad\quad\quad\quad\quad\quad\quad\quad\quad\quad\quad\quad\quad\quad\quad \textbf{3.3}$$

$$S_w = 100\% \text{ and } R_t = R_o \quad\quad\quad\quad\quad\quad\quad\quad\quad\quad\quad\quad\quad\quad\quad\quad\quad \textbf{3.4}$$

Hydrocarbon-bearing zones:

$$\phi = \{a*(R_w/R_t)^{1/m} \quad\quad\quad\quad\quad\quad\quad\quad\quad\quad\quad\quad\quad\quad\quad\quad\quad\quad\quad\quad \textbf{3.5}$$

$$S_w < 1.0 \text{ and } R_t > R_o \quad\quad\quad\quad\quad\quad\quad\quad\quad\quad\quad\quad\quad\quad\quad\quad\quad\quad \textbf{3.6}$$

where; ϕ=Resistivity (conductivity) derived porosity

R_w=Resistivity of formation water at formation temperature

R_o=Formation resistivity when Sw =100%

R_t=True formation resistivity (remember Rt=Ro when Sw=100%)

S_w=Water saturation of uninvaded

a=Constant (Dresser Atlas uses 1.0 for carbonates and 0.62 for sandstones)

m= Constant (Dresser Atlas uses 2.0 for carbonates and 2.15 for sandstones)

The calculated resistivity porosity of water-bearing zones (S_w=1.0) is close to true porosity. However, if hydrocarbons are present, he calculated resistivity porosity will be less than the true porosity. This apparent porosity loss results because hydrocarbons have greater resistivity than formation water. When a porous and permeable water-bearing formation is invaded by drilling fluid, formation water is displaced by mud filtrate.

Porosity in a water bearing formation can be related to shallow resistivity by the following equation

$$S_{xo}=\sqrt{F*R_{mf}/R_{xo}} \quad\quad\quad\quad\quad 3.7$$

Where S_{xo}=1.0 (100% in water bearing zone)

$$1.0=\sqrt{FR_{mf}/R_{xo}} \quad\quad\quad\quad\quad 3.8$$

Solve for F: $F=R_{xo}/R_{mf}$

Remember $F=a/\phi^m$

Therefore, $a/\phi^m=R_{xo}/R_{mf}$ $\quad\quad\quad\quad\quad 3.9$

Solve for porosity (ϕ)

$$\phi=(a*R_{mf}/Rxo)^{1/m}$$

$$\phi=a*R_w/Rt \quad\quad\quad\quad\quad 3.10$$

For the Pate well, porosity value is determined by using (equation 3.10)

Given R_w =0.038, and R_t from the log curve= 6,

a=constant=1 for carbonates

48

and m—constant=2.0 (for carbonates)

Then, $\phi = (1*0.038/6)1/2$

=0.0795*100

Therefore the formation porosity value=7.95

For the rest of the wells, the results obtained are as in table.3.1 below.

Table 3.1: Results for the 7 Wells

Well	Depth (m)	Fm	SP (mv)	Ri (Ω-m)	Rt (Ω-m)	Tf °C	Rm (Ω-m)	Rmf (Ω-m)	Rmc (Ω-m)	Rw (Ω-m)	ϕ
Pate	3200.40-3194.30	Pate Lmst	-8	12	6	119.39	0.081	0.055	0.13	0.038	7.95
Wal merer	3142.49-3124.20	Walu sst	-14	5	9	116.50	0.184	0.051	0.35	0.042	6.50
Walu	3386.33-3389.38	Walu sst	-10	12	8	121.72	0.097	0.0547	0.30	0.041	6.80
Garissa	268.22-265.18	Marafa Fm	-10	6	5	36.61	0.602	0.430	0.85	0.0310	6.42
Kipini	3550.92-3535.68	Kipini sands	-22	9	12	125.72	0.094	0.0532	0.30	0.042	6.00
Ndori	3188.21-3203.45	Pate lmst	-30	2	10	106.94	0.104	0.146	0.35	0.052	7.02
Hagarso	1407.26-1411.83	Hagarso Lmst	-15	3	2	71.72	0.46	0.351	0.543	0.063	17.6

3.5 Stratigraphic Panel/Fence diagram

Panel or fence diagrams are used for graphically representing stratigraphic data in three dimensions. They are similar to cross sections, but rather than interpolating subsurface geology from a map, one interpolates the geology between stratigraphic sections. They are effective at demonstrating changes in lithofacies, pinchouts, truncations, unconformities and other stratigraphic relationships occurring in a region (Margaret, 1960)

3.5.1 Procedure for Constructing Panel/Fence diagram

The source of data for constructing this type of diagram is in appendix, table 2.

The two first steps in constructing a fence diagram were to:

1) Mark the locations of each section on the base map

2) Choose a vertical scale. In this case 1.2 cm representing 500 meters and a horizontal scale of 1.5 centimeters representing 20 Kilometers.

3) The tops of the sections were considered as the lower time sections of the time rock unit. It was then drawn on a vertical line representing the length of the Section and marking off the stratigraphic boundaries along the line.

The next step was to choose pairs of sections between which to draw the "fence" or panels, i.e. the facies and stratigraphic relationships. The selection of panels was based on the relative locations of sections and the lithologic and stratigraphic variations. Where a choice was possible between several sections, selection was made in those, which would present the panel in the most advantageous orientation and would show the widest variation in lithologic and stratigraphic relationships. Most sections were connected to two other sections with panels. Where unconformities are present, a wavy line is drawn to

symbolize them. Once all of the useful panels were completed, the fence diagram resulted

showing the three-dimensional geometry of the various stratigraphic units of the seven

wells considered as shown in (figure 3.5)
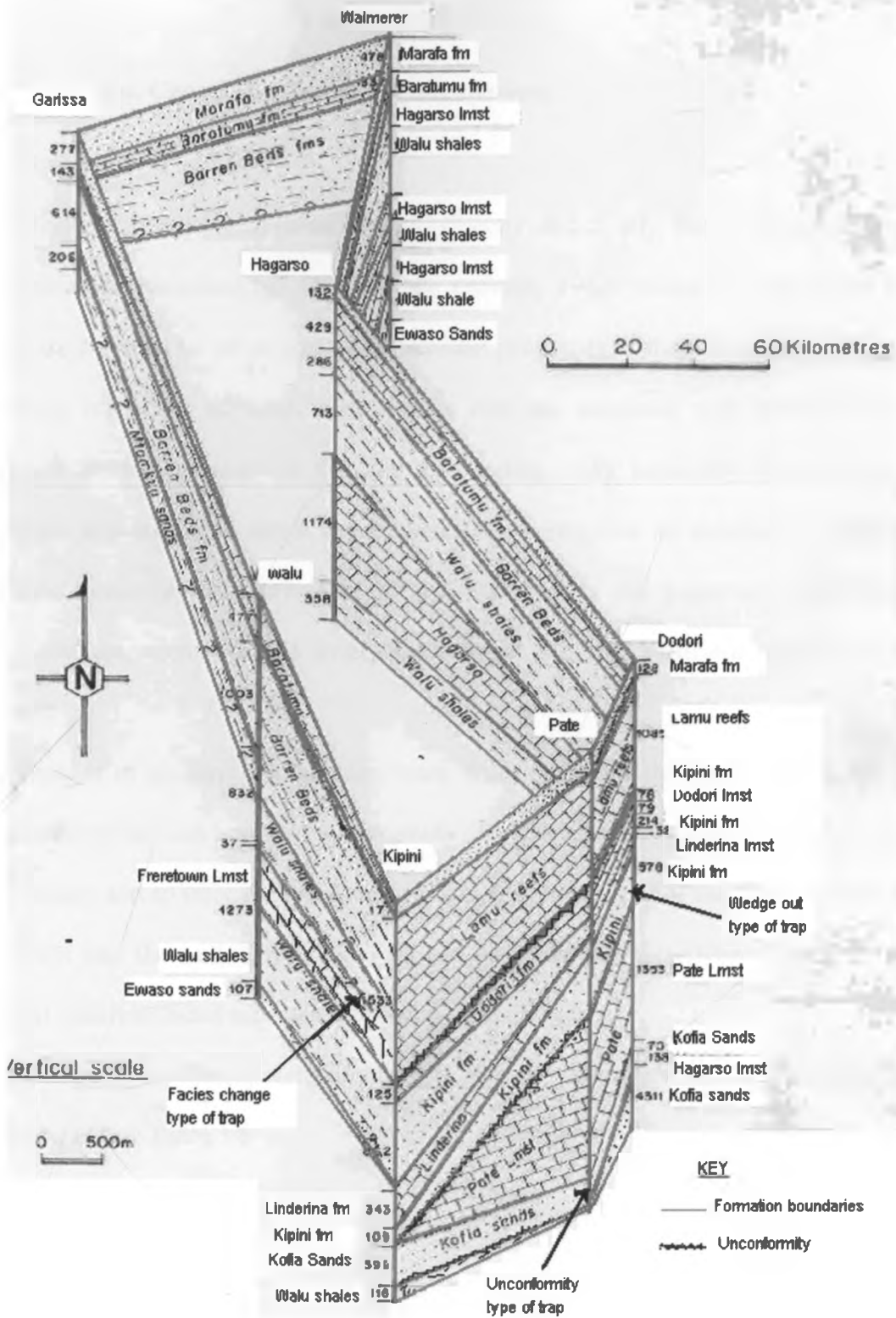
Figure 3.5: Stratigraphic fence showing the stratigraphic relationships for the seven wells

CHAPTER FOUR

4.0 Discussion, Conclusion and Recommendations

4.1 Discussion

The electrical resistivity of rocks depends directly on porosity, pore fluid resistivity, and saturation as determined by Archie's Law (Archie, 1942). When the pore fluids in the rocks are replaced by oil or gas, most physical properties of the rocks are modified with electrical resistivity affected most. Rocks that are saturated with hydrocarbons are normally much more resistive than the surrounding rocks, especially if the surrounding rocks are saturated with saline water, therefore, there exists an excellent possibility for electrical resistivity measurements to indirectly detect the presence of hydrocarbon accumulations, even in subtle stratigraphic traps, provided sufficient resolution can be attained

The process of geophysical well log were done to obtain the properties of the rocks penetrated by the well bore and to determine the capacity of rocks to contain fluids that is the porosity and to infer the permeability, which is the ability of the fluids to flow from formation into the well. The method proved useful as the objectives of the study were realized which included estimation of reservoir parameters

The results of geophysical well log analysis give the porosity values for the seven wells are presented on Table 3.6

Table 3.6: Porosity Values for the 7 Wells

Well	Porosity %	Formation
Pate	7 95	Pate Lmst
Walmerer	6.50	Walu sst
Walu	6.80	Walu sst
Garissa	6 42	Marafa fm
Kipini	6 00	Kipini sands
Dodori	7.02	Pate lmst
Hagarso	17 6	Pate Lmst

From the above table, it can be seen that the porosity values for the seven well range from fair to good as per the interpretation guidelines in petroleum industries where porosity value greater than 40% is termed as excellent, 15-35%, Very good, 10-15% good , 5-10% fair and for anything less than 5 % is termed poor.

Pate Limestone encountered in Hagarso well registered the highest porosity value of 17 6%. This shows that they make good reservoir rocks in accumulating oil and gas . The same formation is also encountered in Pate and Dodori wells where their porosity values are also generally good.

In addition to deducing reservoir capabilities using electric logs, lithology well-log data was also used to construct a fence stratigraphic diagram. This allowed correlation of the formation on the entire area covered by the seven wells and thereby permitting identification of stratigraphic traps for oil and gas. Stratigraphic types of traps are

depositional in nature. This means they are formed in place, usually sandstone ending up enclosed in shale.

From the fence diagram (Figure 3.5), it can be clearly seen that where Kofia sands are overlaid unconformably by the Pate limestone, unconformity type of trap is expected to occur. This is seen in the vicinity of Kipini, Pate and Dodori wells. From the Walu well towards the Kipini well, the Freretown limestones which are laid below and above by the Walu shales are thinned out as they approach the Kipini region. What is expected of such a scenario is the facies change type of stratigraphic trap.

Where Kipini formation overlies Pate limestone and is overlaid by Linderina limestone in the Pate and Dodori well regions, wedge out type of trap is created. Kipini formation is further thinned out towards the Kipini well region and where the formation disappears almost completely, a pinchout type of stratigraphic trap is thus created.

4.2 Conclusion

Exploration for stratigraphic traps in the Lamu basin was done using the method of geophysical well logs. The study involved examining and analyzing spontaneous potential log curves of the selected wells with the aim of evaluation reservoir parameters. The method proved to be the most reliable since it made the properties of the permeable formation to be determined. Also incorporated in the study was the lithology well log data. This type of data was utilized in the construction of fence diagram. The latter was invaluable in graphically assisting in identifying areas or zones which are the possible types of stratigraphic traps.

4.3 Recommendations

Most data acquired from a well can provide information about the formations only in a small radius around that well, while the complete reservoir may extend over several square miles. To accurately portray the reservoir, the interpretation results from all wells drilled into the reservoir should be combined with the seismic data to construct a 3-D model of the reservoir. This model not only portrays the shape of the reservoir, but detail properties of the rocks and fluids as well.

The distance between the considered wells are enormous and hence conclusions made may not reflect what is actually in reality. This calls for more wells to be drilled in the area at closer proximities.

Reference:

Archie, G. E., (1942). The Electrical Resistivity log as an aid in determining some reservoir characteristics: Trans. AIME 146, 54-62.

Asquith, G ,and Gibson, C. R.,(1982). Basic Well Log Analysis for Geologists, American Association of Petroleum Geologists, Tulsa, Oklahoma 74101, USA

Asquith, G, (1990). Log Evaluation of Shaly Sand Reservoirs: A Practical Guide: AAPG Continuing Education Course Note Series 31, 59P

Brooks, J. Fleet A. J. (Eds.) (1987). Marine Petroleum Source Rocks. Geol. Soc. Spec. Publ 26, Blackwell, Oxford, 444p,

Caswell, P.V., (1956) Geology of Kilifi-Mazeras area. Ministry of Environment and Developments In Petroleum Science, 5 Oil Shales. Edited by Teh Fu & George V. C. (1976) Elsevier Scientific Publishing Company

Coffin, M. F. and Rabinowitz P. D, (1988). Evolution Of The Conjugate East African-Madagascar Margins and the Western Somali Basin. Geological Society of America Special Paper, PP. 25.56

Dobrin, M.B., (1960). Introduction to Geophysical Prospecting. 2nd Edition. McGraw Hill Book Company, New York, Toronto, London

Dresser Atlas, (1975). Log Interpretation Fundamentals: Houston, Dresser Industries, Inc.

Edwards, D.P., Lacour-Gayet, P J and Suan, J., (1963). Log Evaluation in Wells drilled with inverted oil emulsion mud SPE 1020y, San Anthonio. Pp.313-318

Frick, T.C., (1962). Petroleum Production Handbook, McGraw-Hill Publishers, New York. PP.19-22.

Gerhard Einsele (1992). Sedimentary Basins, Evolution, Facies and Sediment Budget Springer-Verlog Berlin Heidelberg 1992 printed in German. PP. 571

Hobson, G.D., and Tiratsoo, E.N., (1975). Petroleum Geology. Scientific Press Ltd. Beaconstield, England

Hubbert, M. K., (1956). Drilling and Production Practice, American Petroleum Institute, a Washington, DC, M. K. Hubbert, (1967). American Association of petroleum Geologists (AAPG). Bull. 51, 2207

Jerome, G.M., (1977). Nuclear Methods in Mineral Exploration and Production. Edited by Jerome G. Moise, Elsevier Scientific publishing Co. Amsterdam – Oxford New York 1977 pp. 201.

Kent, P E., and Perry, J.T, (1973). Development of Indian Ocean margin in Tanzania In Blant (Ed.) Sedimentary Basin of East African Coast 2, 113-131.

King, R E., (1972). Stratigraphic Oil and Gas fields. Classification, Exploration Methods, and Case Histories published jointly by the AAPG and the Society of Exploration Geophysicists, Tulsa, Oklahoma, USA., 1972.

Levorsen, A.I., (1960). Paleogeologic Maps. W H Freeman & Co. San Francisco and London

Margaret, S. B., (1960). Subsurface Mapping. John Wiley & Sons Incl. Printed in USA pp 149.

Markorviskii N. l., (1973). Paleogeographic Principles of Oil and Gas Prospecting. John Wiley and Sons. New York, Toronto

Macquillin, R , (1977). Exploring the Geology of Shelf seas. Published by Graham and Trotman Limited

Nettleton, L L., (1940). Geophysical Prospecting for Oil. McGraw Hill Book Company, New York, Toronto, London.

NOCK, (1999). Petroleum Exploration Opportunities in the Lamu Basin of S. East Kenya, North and 4 Data scan, Nairobi pp9

North, F. K., (1984) Petroleum Geology. Allen and Uwin Hyman, London and Sidney

Nyagah, K., (1993). Stratigraphy, Depositional History and Environments of Deposition of Cretaceous – Tertiary strata in the Lamu Basin, S.E. Kenya and implication on Hydrocarbon Exploration. Proceed 5th Conference. Geology of Kenya. Feb. 1993. Pp 110-115; Nairobi.

... 1994: Stratigraphy, Depositional History and Environment of Deposition of Cretaceous through Tertiary strata in the Lamu basin, S.E. Kenya and Implication on Reservoirs for the exploitation-sediment. Geol. 96, pp.43-71, Amsterdam.

Parasnis, D.S., (1977). Principles of Applied Geophysics, 5th Edition. Chapman and Prentice Hall

Pirie, R G., (1977). Oceanography Contemporary Reading in Ocean Sciences. 2nd Edition Network, Oxford University Press.

Pirson, S.J., (1963). Handbook of Well Log Analysis for Oil and Gas formation Evaluation. Prentice-Hall Inc.,Englewood Cliffs,New Jersey, pp 42 – 43.

Richard, E.C., (1973). Petroleum Geology, A Concise Study. Elsevier Scientific Publishing Company. Amsterdam, the Netherlands.

Richard H. M., (1979), Well log Formation Evaluation, AAPG continuing education Course note series #1422.

Schlumberger (1989). Log interpretation Principles/ Applications Schlumberger Educational services 5000 Gulf Freeway Houston, Texas, 77023. PP5-12

Schlumberger Limited, (1969a). Log Interpretation Principles. Schlumberger Limited, 277 Park Avenue New York, N.Y.10017, 110p

_____ (1969b). Log Interpretation Charts. Schlumberger Limited, Houston Texas, 76p.

Schluter, T., (1997). Geology of East Africa .Gebrüder Borntrager, Berlin Stuttgart Printed in Germany by Druckerei Zu Altenburg pp. 253.

Selley, R.C., (1985). Elements of Petroleum geology. Freeman & Co. New York pp. 15-65

Sheriff, R.E., and Lloyd, P. Geldart, (1995). Exploration Seismology Cambridge University Press, Cambridge.

Simiyu M. S., (1989). Geophysical, Stratigraphy and Structure of Lamu embayment. Unpublished M.Sc. thesis, University of Nairobi.

Smolen, J.J., (1977). Formation Evaluation Using Wireline Formation Tester Pressure
Data SPE 6822, Denver. PP 4-8

UNEP (1998) Eastern Africa Atlas of Coastal Resources.

Wallace, E. Pratt., and Dorothy Good., (1950). World Geography of Petroleum
Copyright, 1950, by American Geographical Soc. London. Geoffrey Cumberlege,
Oxford University Press.

Walters, R., and Linton, R E., (1972) The Sedimentary Basin of Coastal Kenya – in
Basin Sediment. Litt. Africaine 2nd littoral Austral-Oriental Sympos. Montreal
(1972) Association. Serv Geol. Afrique, 133-158, Paris.

Appendices

Appendix 1: TABLES

Table 1: Results for the 7 Wells

Well	Depth (m)	Fm	SP (mv)	Ri (Ω-m)	Rt (Ω-m)	Tf °C	Rm (Ω-m)	Rmf (Ω-m)	Rmc (Ω-m)	Rw (Ω-m)	ϕ
ate	3200.40-3194.30	Pate Lmst	-8	12	6	119.39	0.081	0.055	0.13	0.038	7.95
Val merer	3142.49-3124.20	Walu sst	-14	5	9	116.50	0.184	0.051	0.35	0.042	6.50
Valu	3386.33-3389.38	Walu sst	-10	12	8	121.72	0.097	0.0547	0.30	0.041	6.80
arissa	268.22-265.18	Marafa Fm	-10	6	5	36.61	0.602	0.430	0.85	0.031	6.42
ipini	3550.92-3535.68	Kipini sands	-22	9	12	125.72	0.094	0.0532	0.30	0.042	6.00
odori	3188.21-3203.45	Pate lmst	-30	2	10	106.94	0.104	0.146	0.35	0.052	7.02
agarso	1407.26-1411.83	Hagarso Lmst	-15	3	2	71.72	0.46	0.351	0.543	0.063	17.6

Table 2: Lithologic Well-log Data

Table 2(i): Dodori-1 Well
Latitude   01°48' 53.7"S   Longitude   41°11' 4"E
Elevation KB (M)   32   Ground level/water depth (M) 26   Total   depth   drilled
(M)   4311   Total depth drilled (M) subsea   4279
Megasequence boundaries

Megasequence	Depth KB (M)	Subsea (M)	Thickness (M)
Megasequence IV	Surf	32	1213
Megasequence III	1213	-1181	2334
Megasequence II	3547	-3515	764
Formation tops			
Marafa Formation	Surf	32	128
Lamu reefs	128	-96	1085
Kipini formation	1213	-1181	25.56

Dodori limestone	1291	-1259	79
Kipini formation	1370	-1338	214
Linderina limestone	1584	-1552	32
Kipini formation	1616	-1584	525.56
Pate limestone	2194	-2162	1353
Kofia sands	3547	-3515	70
Hagarso limestone	3617	-3585	138
Kofia sands	3755	-3723	556
Paleo tops			
Quaternary/Late Pliocene (Unconf in Lower Pliocene)	surf		
Upper Miocene	128		
Middle Miocene	286		
LateMiocene(Unconf inUpper ligocene)	831		
Lower Oligocene	1185	-1153	40
Upper Eocene	1225	-1193	152
Middle Eocene	1325.56	-1346	1332
Lower Eocene	2710	-2625.56	826
Paleocene	3536	-3504	775

Table 2(ii): Walu-2 Well
Latitude   01⁰ 38' 02" S   Longitude   40⁰ 15' 10" E
Elevation KB (M)   92   Ground level/water depth (M)   86
Total depth drilled (M)   3729   Total depth drilled (M) subsea   -3637
Megasequence boundaries

Megasequence	Depth KB (M)	Subsea (M)	Thickness (M)
Megasequence IV	Surf	92	477
Megasequence III	477	-385	1003
Megasequence II	1426.67	-1388	2249
Formation tops			
Baratumu Formation	Surf	92	477
Barren Beds formation	477	-385	1003
Walu shales	1426.67	-1388	832
Freretown Lmst	2312	-2220	37
Walu shales	2349	-2257	1273
Ewaso sands	3622	-3530	107
Paleo tops			
Quaternary/Late Pliocene	surf	92	6

(Unconf in Lower Pliocene)			
Upper Miocene	6	86	67
Middle Miocene	73	193	44
Late Miocene(Unconf. in Upper Oligocene)	417	-325	60
Oligocene	477	-325	60
Upper Eocene(Unconf in Upper Paleocene)	628	-536	851
Santonian	1479	-1387	322
Turonian	126.671	-1709	193
Cenomanian	1994	-132.222	450
Albian	2444	-2352	1174
Aptian	3618	-3526	111

Table 2(iii): Wal merer-1 Well
Latitude   00^0 06' 35" S Longitude   40^0 35' 05" E
Elevation KB (M)   152   Ground level/water depth (M)   148
Total depth drilled (M)   3794   Total depth drilled (M) subsea   -3640
Megasequence boundaries

Megasequence	Depth KB (M)	Subsea (M)	Thickness (M)
Megasequence IV	Surf	154	815
Megasequence III	815	-661	655
Megasequence II	1470	1316	2324
Formation tops			
Marafa Formation	Surf	154	425.56
Baratumu Formation	425.56	-324	337
Barren Bed formation	815	-661	655
Hagarso limestone	1470	-1316	131
Walu shales	1601	-1447	105
Hagarso limestone	1706	-1552	196
Walu shales	132 222	-1748	143
Hagarso limestone	2045	-1891	33
Walu shales	2025.56	-1924	19
Ewaso sands	2097	-1943	1697
Paleo tops			
Quaternary/Late Pliocene	surf	154	273
MiddleMiocene(Unconf.in Upper/Oligocene)	273	-119	605
Late Oligocene	825.56	-724	592
Albian	1470	-1316	627
Aptian	2097	-1943	251
Neocomian	2348	-2194	1446

Table 2(iv): 4. Hagarso Well
Elevation KB (M) 92 Ground level/water depth (M) 85
Total depth drilled (M) 3092 Total depth drilled (M) subsea -3000

Megasequence boundaries

	Depth KB (M)	Subsea (M)	Thickness (M)
Megasequence IV	Surf	92	561
Megasequence III	561	-469	286
Megasequence II	847	-735	2245
Formation tops			
Marafa Formation	Surf	94	132
Baratunu Formation	132	-40	429
Barren Bed formation	561	-469	286
Walu shales	847	-755	713
Hagarso limestone	1560	-1468	1174
Walu shales	2734	-2642	358
Paleo tops			
Quaternary/Late Pliocene (Unconform. in Late Pliocene)	Surf	92	132
Upper Miocene (Unconf. Upper Oligocene.)	132	-40	432.22
Late Oligocene(unconformity in Upper Eocene)	622	-530	216
Coniacian	838	-746	305
Turonian	1143	-1051	247
Cenomanian	1332.22	-1298	225
Albian	1615	-1523	1134
Aptian	2749	-2657	343

Table 2(v): Kipini-1 Well
Latitude 02⁰ 29' 24" S Longitude 40⁰ 35' 52" E
Elevation KB (M) 23 Ground level/water depth (M) 17
Total depth drilled (M) 3663 Total depth drilled (M) subsea -3640
Megasequence boundaries

Megasequence	Depth KB (M)	Subsea (M)	Thickness (M)
Megasequence IV	Surf	23	1710
Megasequence III	1710	-1687	1439
Megasequence II	3149	-3126	514
Formation tops			
Marafa Formation	Surf	23	177
Lamu reefs	177	-154	1533

Dodori limestone	1710	-1687	125
Kipini Formation	1835	-1812	862
Linderina limestone	2697	-2674	343
Kipini Formation	3040	-3017	109
Kofia sands	3149	-3524	398
Walu shales	3547	-3524	116
Paleo tops			
Quaternary/ Pliocene (Uncont. in Lower Pliocene)	Surf	23	176
Upper Miocene	176	-154	134
Middle Miocene	310	-287	26.679
Lower Miocene (unconf in the Lower Oligocene)	1119	-1096	582
Lower Oligocene	1701	-1625.56	71
Upper Eocene	1772	1749	315
Middle Eocene (Unconform. in Upper Paleocene)	2087	-2064	1068
Maestrichtian/Campanian)	3155	-3132	508

Table 2(vi): Garissa-1 Well
Latitude   00° 21' 04" S Longitude   332.22 48' 43" E
Elevation KB (M)   231   Ground level/water depth (M)
Total depth drilled (M)   1240   Total depth drilled (M) subsea   -1009
Megasequence boundaries

| Megasequence	Depth KB (M)	Subsea (M)	Thickness (M)
Megasequence IV	Surf	231	420
Megasequence III	420	-189	614
Megasequence II	1034	-26.673	206
Formation tops			
Marafa Formation	Surf	231	277
Baratumu formation	277	-46	143
Barren Beds Formation	420	-189	614
Mtomkuu shales	1034	-26.673	206
Paleo tops			
Quaternary/ Pliocene (Unconf. in Lower Pliocene)	Surf		
Middle Miocene	99	-132	289
Lower Miocene (Unconf. in Upper Oligocene)	388	-157	124
Oligocene (Unconf. in Jurassic)	512	-281	522
Jurassic	1034	-26.673	206

Table 2(Vii): Pate-1 Well
Latitude   02⁰ 03' 50" S Longitude   41⁰ 05' 00" E
Elevation KB (M)   8   Ground level/water depth (M)   2
Total depth drilled (M)   4188   Total depth drilled (M) subsea   -4126.67

Megasequence boundaries

Megasequence	Depth KB (M)	Subsea (M)	Thickness (M)
Megasequence IV	Surf	8	1246
Megasequence III	1246	-1238	2942
Formation tops			
Marafa Formation	Surf	8	162
Lamu reefs	162	-154	1084
Kipini Formation	1246	-1238	79
Dodori limestone	1325	-1317	154
Kipini Formation	1479	-1471	164
Linderina Formation	1643	-1635	189
Kipini Formation	1832	-1824	522
Pate Limestone	2354	-2346	1588
Kipini Formation	3942	-3934	246
Paleo tops			
Quaternary/ Pliocene (Unconf. in Lower Pliocene)	Surf	8	177
Upper Miocene	177	-169	158
Middle Miocene	335	-327	529
Lower Miocene (unconf. in the Upper Oligocene)	864	-856	352
Lower Oligocene	1216	-1208	49
Upper Eocene	1265	-1257	186
Middle Eocene	1433	-1425	1701
Lower Eocene	3134	-3126	1054

Appendix 2: Well log Curves
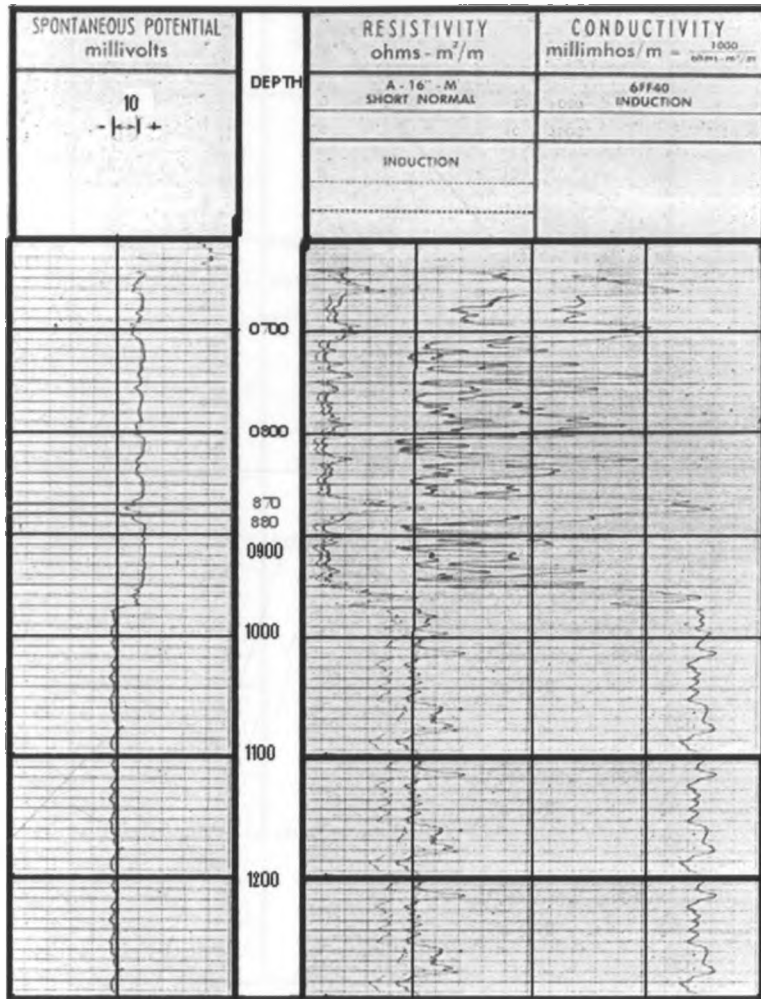
Log Data for Garissa well

Figure 2.1: Log Curve for Garissa Well
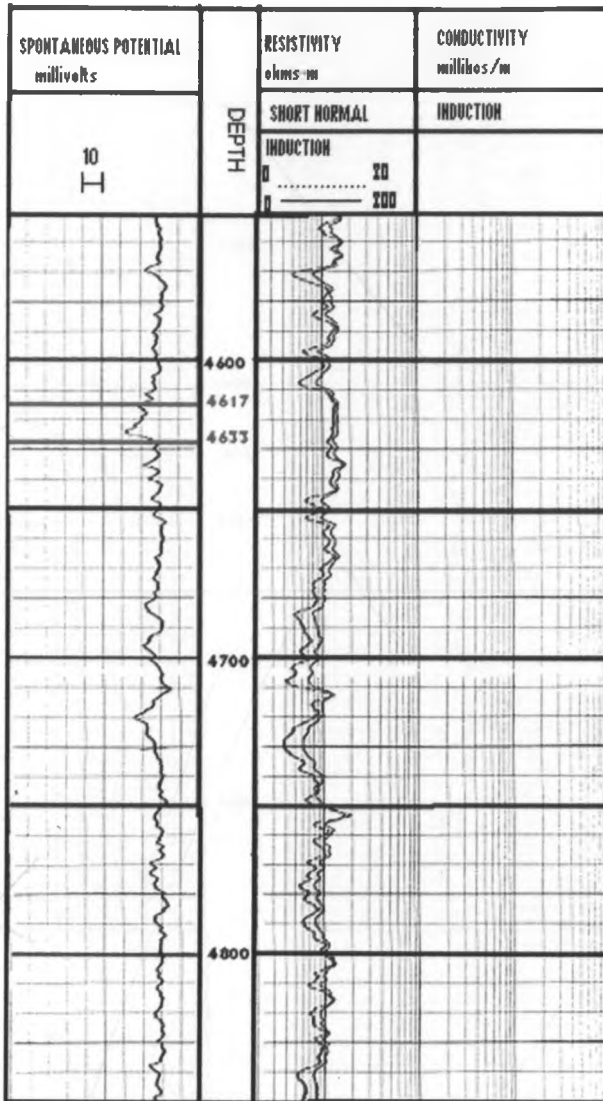
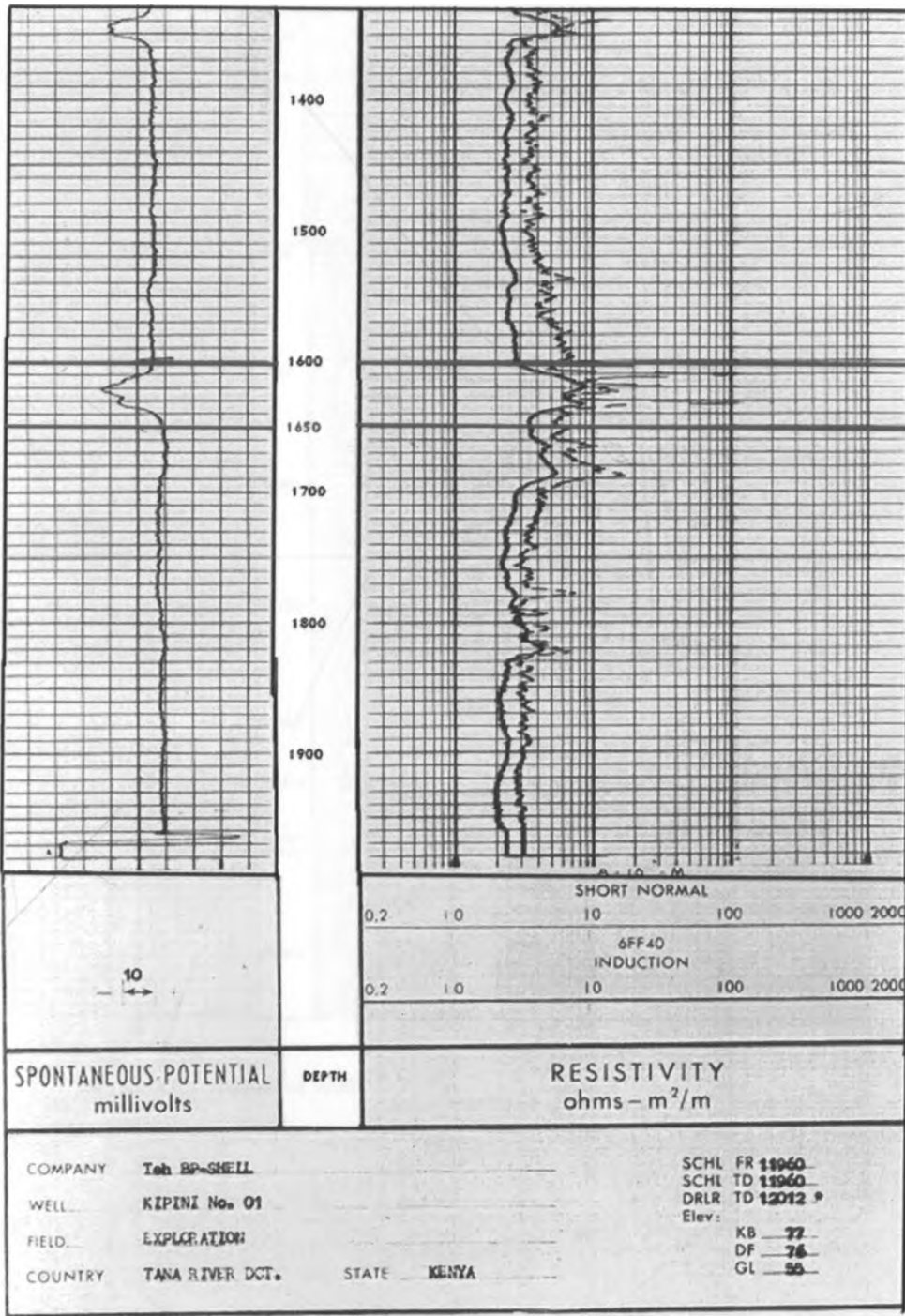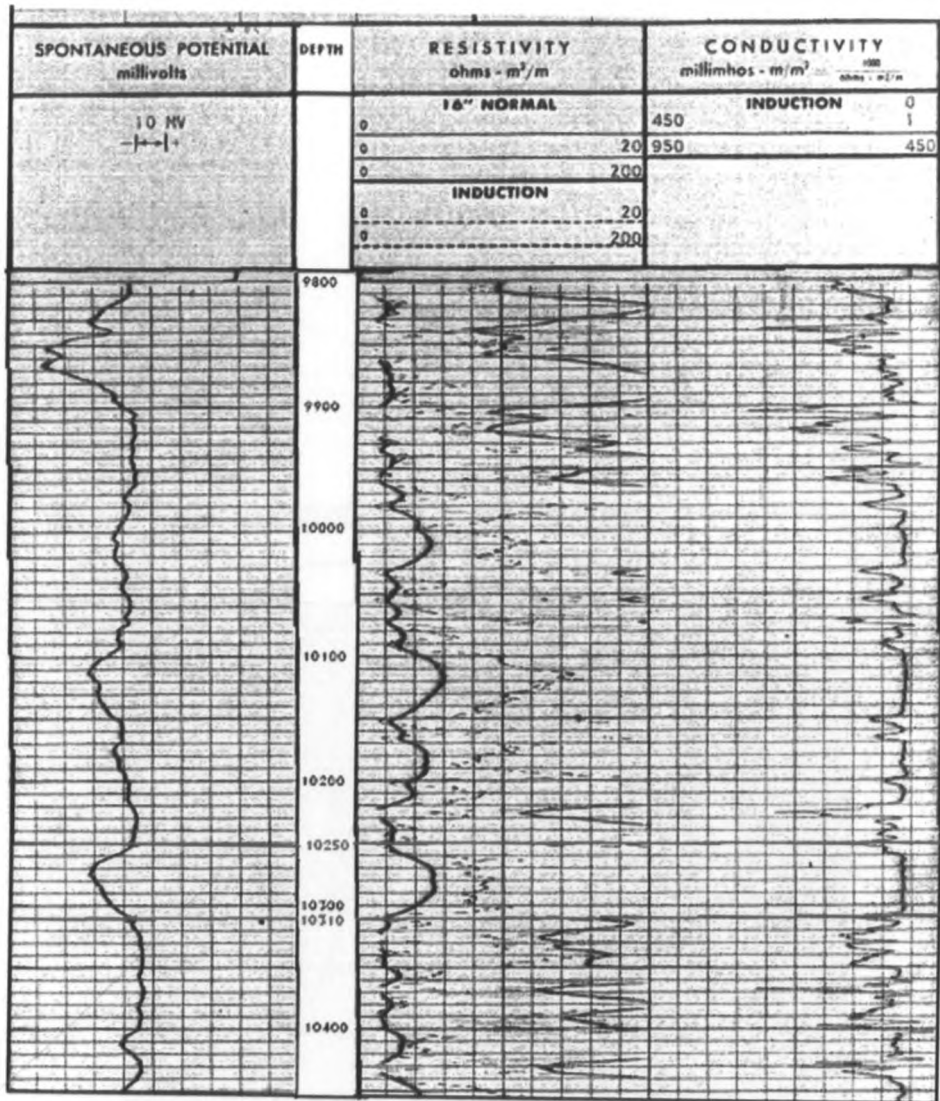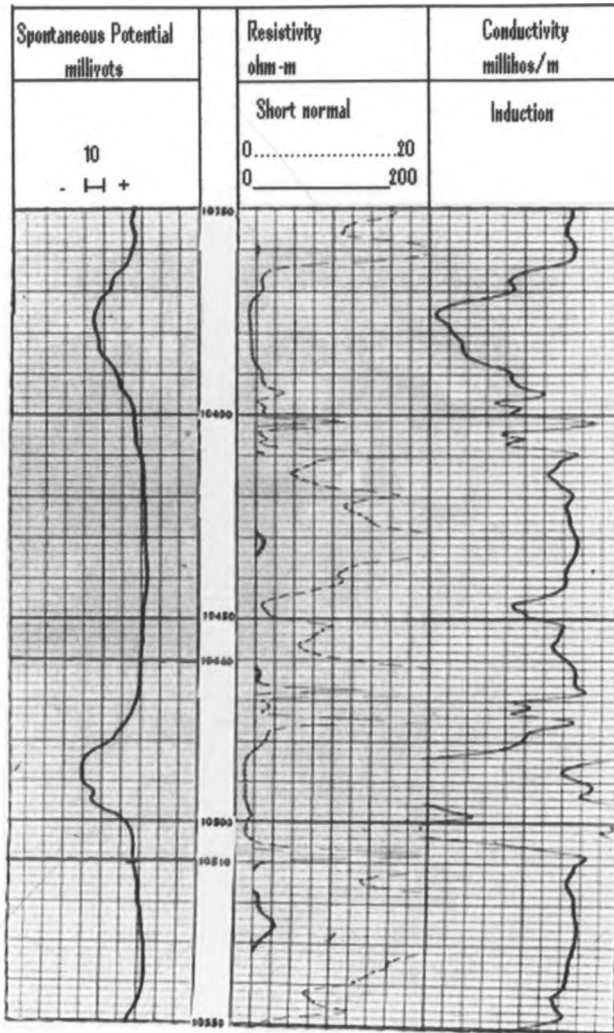Log data for Hagarso Well

Figure 2.2: Log Curve for Hagarso Well

Figure 2.3 : Log Curve for Kipini Well

Log data for Walmerer well

Figure 2.4 : Log Curve for Walmerer Well

Well Log data for Walu well

Figure 2.5: Log Curve for Walu Well

Log data for Dodori well

Figure 2.6 : Log Curve for Dodori Well